

# Ireteba Pluton, Eldorado Mountains, Nevada: Late, Deep-Source, Peraluminous Magmatism in the Cordilleran Interior

Jessica D'Andrea Kapp,<sup>1</sup> Calvin F. Miller,<sup>2</sup> and Jonathan S. Miller<sup>3</sup>

Department of Geology, Vanderbilt University, Nashville, Tennessee 37235, U.S.A.  
(e-mail: jessica@oro.ess.ucla.edu)

## ABSTRACT

The Ireteba pluton is a ~66 Ma biotite ± muscovite ± garnet granite emplaced at the eastern edge of the Cordilleran plutonic belt in southeastern Nevada. In common with other Cordilleran peraluminous granites, its mineralogy, major element chemistry, isotopic composition, and abundant Proterozoic zircon inheritance document crustal origin. Distinctive trace element chemistry, field relations, and inherited components further constrain its genesis. High Sr concentrations, low heavy rare earth elements, and absence of negative Eu anomalies indicate that the Ireteba magma was extracted from a residue relatively rich in garnet and poor in feldspar; rounded quartz is probably a resorbed, high-P liquidus phase or restite. The granite shares with adakites (slab-derived arc magmas) and Archean granitoids the Sr–rare earth element signature of deep-source origin. Nd–Sr isotopic compositions indicate a dominantly crustal origin for the granite, but it is less mature than the underlying ancient Mojave crust. The granite is apparently a hybrid derived primarily from the ancient crust but with a less mature component as well: either Jurassic igneous rock, as suggested by sparse 150–170 Ma zircon cores, or juvenile mafic magma, as implied by abundant synplutonic mafic rocks, or both. Influx of basaltic magma during the waning stages of Cordilleran convergence may have triggered melting in the deep, thickened crust, with basaltic magmas being trapped beneath the less dense crustal melts. Like other relatively young peraluminous granites of the Cordilleran Interior, including the Idaho-Bitterroot batholith, the Ireteba pluton may reflect changing conditions during the waning stages of plutonism.

## Introduction

Strongly peraluminous granitoid rocks are generally interpreted to have been derived from mature continental crust, and in many cases they are attributed to metasedimentary sources (“S-type” granites; Pitcher 1993). In the western North American Cordillera, strongly peraluminous granites are common in a broad inland belt that stretches from southern Canada to northern Mexico (fig. 1; Miller and Bradfish 1980). These granites are principally of late Mesozoic age, but in the northwestern United States and adjacent British Columbia and in Arizona and adjacent Sonora, peraluminous plutonism continued into the early Paleogene (Miller and Barton 1990). In contrast to many other per-

aluminous plutonic belts, continental collision does not appear to have been involved in the generation of the Cordilleran Interior granites, and their distribution and age suggest a relationship to subduction off the western margin of North America. The importance of chemically mature sedimentary source material in production of the Cordilleran granites has been strongly questioned (Miller 1985; White et al. 1986; Miller and Barton 1990), but, in common with most peraluminous granites worldwide, these intrusions are generally interpreted to have been produced by crustal anatexis.

The Ireteba granite in Nevada is petrographically typical of the peraluminous intrusions of the Cordilleran Interior and shares with them indisputable evidence for crustal source material. However, its field relations and geochemistry differ from what has been considered typical. The granitic magma interacted extensively with mafic magma in the deeper portions of the pluton; its trace element

Manuscript received September 18, 2001; accepted January 31, 2002.

<sup>1</sup> Present address: Department of Earth and Space Sciences, University of California, Los Angeles, California 90095-1567, U.S.A.

<sup>2</sup> E-mail: millercf@ctrvax.vanderbilt.edu.

<sup>3</sup> Department of Geology, San Jose State University, San Jose, California 95192-0102, U.S.A.

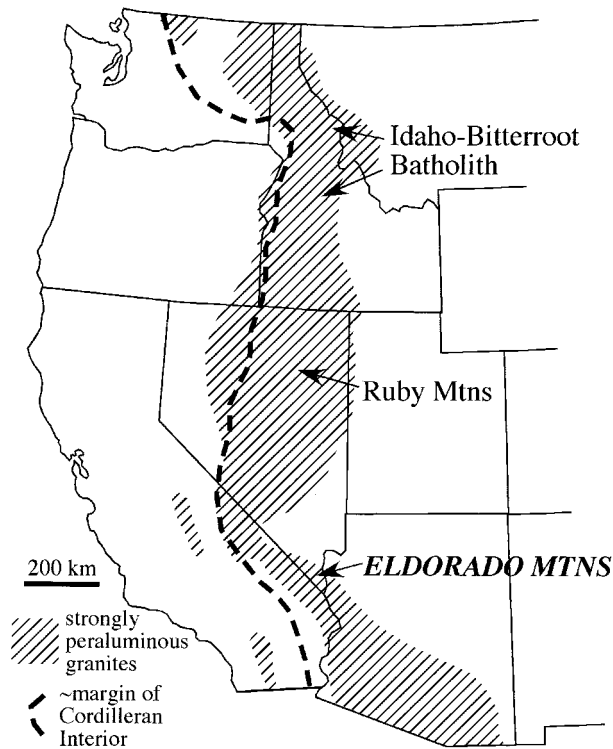


**Figure 1.** Distribution of strongly peraluminous granitoids and Cordilleran Interior plutonism, western United States (modified from Miller and Barton 1990). The Eldorado Mountains, where the Ireteba pluton is located, are shown for reference (see figs. 2, 3).

characteristics are more akin to “adakites” (deep-source felsic magmas; Drummond and Defant 1990) than to those of most reported peraluminous granites; and its isotopic composition, though highly evolved, is more consistent with hybrid than purely crustal origin. Furthermore, its latest Cretaceous–earliest Paleogene age is distinctly younger than those of most Cordilleran intrusions at the same latitude. In this article we describe the Ireteba granite, evaluate its petrogenesis, and propose that its origin is unusual or, more likely, it reflects processes that may be important but underappreciated elsewhere in the Cordillera and worldwide.

### Geologic Setting

The Ireteba pluton is exposed in the central to southern Eldorado Mountains of southernmost Nevada (fig. 2). The Eldorado Mountains lie along the northern Colorado River Trough, a topographic depression formed during Basin and Range-related rifting that occurred between 16 and 10 Ma at this latitude (Faulds et al. 1990). This crustal extension

was accompanied by intense magmatism and extreme tilting of large crustal blocks. Based on studies of the surrounding Miocene plutons, the current exposures of the Ireteba pluton were about 5–13 km deep at 16 Ma, shallowest in the north and deepest in the southeast (Falkner et al. 1995; Patrick and Miller 1997; Bachl et al. 2001).

The basement complex of the northern Colorado River Trough includes Early Proterozoic supra-crustal gneisses and Early to Middle Proterozoic orthogneisses interpreted to represent both the Mojave and Arizona crustal terranes (Bennett and DePaolo 1987; Wooden and Miller 1990). The surface exposure of the terrane boundary is thought to lie just to the east of the Eldorado Mountains, across the Colorado River (fig. 2). The metamorphic rocks of the Mojave terrane are generally higher

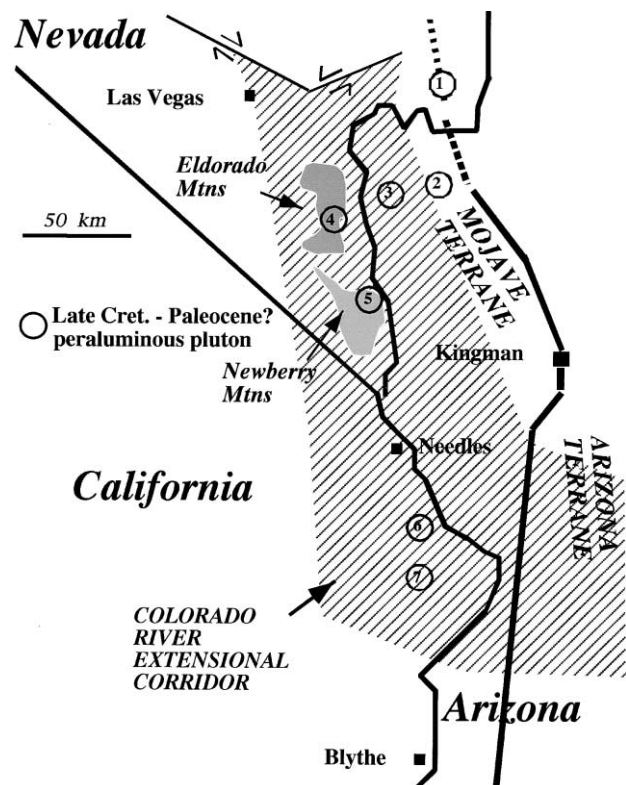


**Figure 2.** Southernmost Nevada and adjacent Arizona and California, showing location of Ireteba pluton and Eldorado Mountains. Late Cretaceous–Paleocene peraluminous plutons: 1, Gold Butte region, Nevada (Fryxell et al. 1992); 2, White Hills, Arizona; 3, Black Mountains, Arizona; 4, Ireteba pluton, Eldorado Mountains; 5, White Rock Wash pluton, Newberry Mountains, Nevada (Ramo et al. 1999); 6, Chemehuevi Mountains, California (John and Wooden 1990); 7, Whipple Mountains, California (Anderson and Cullers 1990).

grade, include more chemically mature sedimentary rocks, and are older than the rocks of the Arizona terrane. Zircon crystallization ages in the Mojave terrane are commonly greater than 1.7–1.75 Ga, with inherited and detrital ages reaching 2.5 Ga; the average crustal formation age based on Nd and Pb isotopes is ~2.0–2.2 Ga (Wooden et al. 1988, 1994; Bennett and DePaolo 1987). In contrast, the Arizona crust appears to have formed entirely after ~1.8 Ga (Bennett and DePaolo 1987; Wooden et al. 1988; Wooden and Miller 1990). Similar 1.4–1.5 Ga, largely undeformed granites are common in both terranes.

The Ireteba pluton lies near the eastern edge of the Mesozoic–early Paleogene Cordilleran intrusive belt of western North America (fig. 1). Exposed Cordilleran plutons are very sparse in the northern Colorado River Trough. All are at least in part strongly peraluminous and all are of known or probable latest Cretaceous–early Paleogene age. The White Rock Wash pluton, exposed in the Newberry Mountains immediately south of the Eldorado Mountains (fig. 2), appears to be essentially identical to the Ireteba granite in geochemistry, petrographic characteristics, and age (Haapala et al. 1996; Ramo et al. 1999; J. D'Andrea and C. F. Miller, unpublished data). The Mesozoic intrusive belt becomes volumetrically important within 20–40 km to the west, where Cretaceous peraluminous and metaluminous and Jurassic metaluminous plutons are abundant (Anderson and Rowley 1981; Miller and Barton 1990; Gerber et al. 1995).

Although the Mesozoic intrusive belt was a consequence of plate convergence and subduction, the style of tectonism differed drastically in time and space during the 100+ m.yr. of magmatism. The Late Cretaceous appears to have been a time of dramatic tectonic transition. By the end of the Cretaceous, plutonism had ceased and there is evidence for extensional tectonism in many parts of the United States Cordillera (Hodges and Walker 1992), including the eastern Mojave Desert (Carl et al. 1991). It has also been suggested that shallow subduction terminated magmatism and cooled the Cordilleran lithosphere at this time (Dumitru 1990).

### Field Relations and Petrography

The Ireteba pluton intrudes Proterozoic gneisses, is cut by the middle Miocene Searchlight and Aztec Wash plutons (Falkner et al. 1995; Bachl et al. 2001), and is overlain by Quaternary alluvium (fig. 3). A few small (<1 m) xenoliths of Ireteba granite are exposed in the adjacent 16.5 Ma Searchlight pluton

within meters of the contact. In contrast, large blocks (up to hundreds of meters) of Ireteba granite are incorporated into the southeastern section of the 15.7 Ma Aztec Wash pluton. The southeastern part of the Ireteba pluton has a weak to strong, dominantly linear ductile fabric. A band of highly deformed, in some places mylonitic, granite extends southward from the southeast corner of the main mass, east of the Searchlight pluton, and underlies the east-dipping Dupont Mountain detachment fault (fig. 3). Elsewhere, the pluton is undeformed.

The Ireteba pluton has sharp but irregular intrusive contacts with the Proterozoic gneisses that constitute its country rock. Pegmatitic dikes emanating from Ireteba granite penetrate as far as tens of meters into the gneiss. Sparse, small (centimeters to meters) xenoliths of gneiss in the granite are limited to areas within meters of the contacts.

The major minerals of the granite are (in order of abundance) plagioclase, quartz, K-feldspar, biotite, muscovite, and in some cases garnet. Accessory minerals include opaques (magnetite ± ilmenite), apatite, zircon, and monazite. Sparse chlorite and rare fibrolitic sillimanite (present in the deformed granite in the initially deepest southeastern area) are interpreted to be secondary. Subhedral to euhedral plagioclase is weakly zoned. A distinctive feature of the granite is the presence of large (~4–8 mm), ovoid quartz grains that are nearly ubiquitous except in the most felsic or deformed rocks. In thin section, these large grains are revealed to comprise multiple subgrains, often with sutured internal boundaries. K-feldspar is commonly present as centimeter-sized phenocrysts, with concentric zoning visible in hand sample. Ubiquitous, subhedral to euhedral biotite is often intergrown with muscovite and is locally altered to chlorite. Subhedral to euhedral primary muscovite is seen in almost every thin section but is not evident in outcrop in some areas. Garnet is present in the most felsic rocks, especially in aplite dikes.

In the southeastern (deeper) region of the pluton, there is widespread field evidence for interaction between granitic and mafic magmas. Interaction is marked (fig. 4) by (1) coherent mafic dikes with very small felsic injections from the surrounding granite, (2) disaggregated mafic dikes with granite filling in gaps, and (3) extensive, highly heterogeneous areas, meters to tens of meters across, consisting of angular, coarse-grained mafic blocks, rounded mafic pods, and occasional fine-grained mafic pillows with crenulate margins, all engulfed in granite. The mafic rocks are fine grained, with abundant

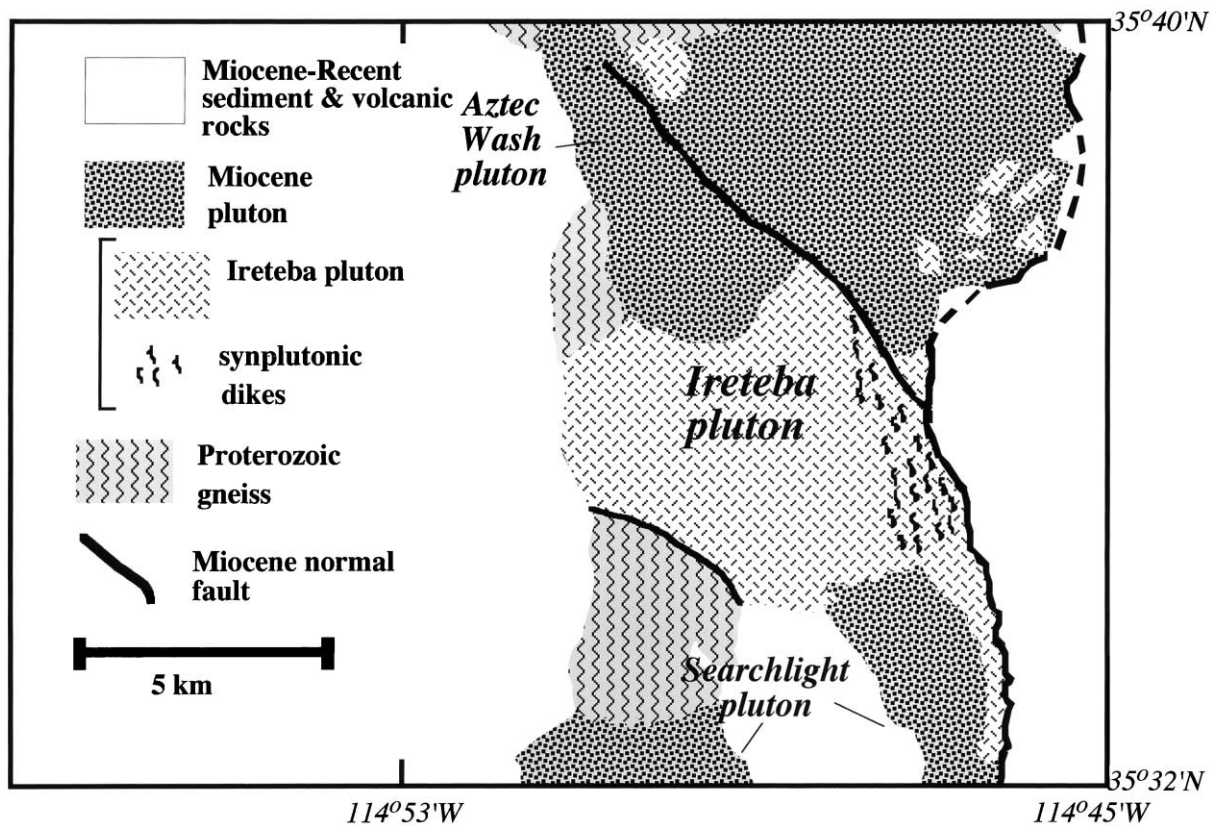


Figure 3. Ireteba pluton and its surroundings

plagioclase and hornblende and lesser amounts of biotite and in some cases clinopyroxene and minor sphene. Material of intermediate composition is locally present between mafic rock and granite, suggesting small-scale mixing. Some of the granite has abundant, tiny (millimeters to centimeters) mafic enclaves that appear to have been derived from adjacent mafic material. Mafic dikes that have sharp contacts with the granite and lack any evidence for hybridization or reinjection by granitic magma are common in some areas (east side of the pluton and in the roof pendant at the northern edge of the Aztec Wash pluton). These dikes clearly postdate solidification of the granite and are probably of Miocene age, although it is possible that they represent the final stages of mafic intrusion that accompanied emplacement of the Ireteba pluton. It is noteworthy that, except in the vicinity of the synplutonic mafic injections, mafic enclaves are absent within the pluton.

#### Analytical Methods

Fresh samples powdered in an alumina ceramic shatterbox were used for major and trace element

and Sr, Nd, and O isotopic analyses; feldspar separates from crushed samples were used for Pb isotopic analyses.

Major and trace element analyses were performed by XRAL Activation Services using X-ray fluorescence (XRF), inductively coupled plasma mass spectrometry (ICP-MS), instrumental neutron activation analysis (INAA), and direct current plasma spectroscopy (DCP). Analysis for Sr, Nd, and Pb isotopes followed procedures described in J. S. Miller et al. (2000), with the exception of sample IR20 (previously analyzed by J. L. Wooden at the U.S. Geological Survey, Menlo Park, Calif.). Oxygen isotope ratios were determined by Geochron Laboratories for six whole-rock powders and two quartz separates. The separates were picked by hand from crushed rock samples.

Zircon was separated from fresh samples and mounted in epoxy with fragments of a zircon standard. The grains were then "mapped" by backscattered electron imaging (JEOL 733 Superprobe, Rensselaer Polytechnic Institute) to guide selection of analytical points on the Cameca ims 1270 ion microprobe at the University of California, Los An-

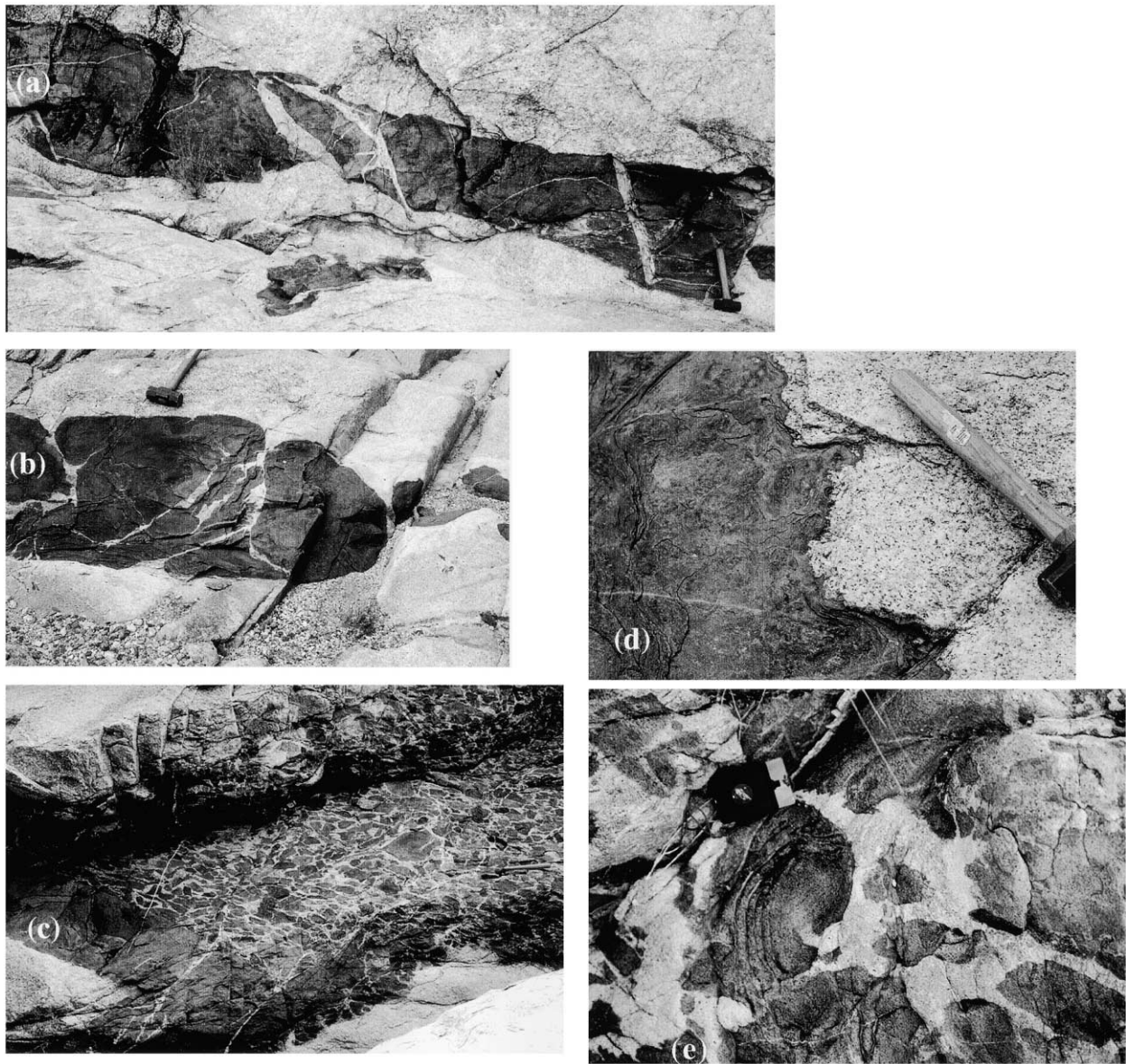


**Figure 4.** Field relations between granite and mafic rocks in the Ireteba pluton. *a–c*, Disaggregated mafic dikes hosted by granite. *d*, Crenulate contact between fine-grained mafic dike and granite. *e*, Mafic pillows, contaminated granite matrix.

geles. Ion microprobe techniques follow those described in Quidelleur et al. (1997) and C. F. Miller et al. (2000). The ion beam was focused to a  $15 \times 20$ -micron ellipse. Zircon AS3 ( $1099.1 \pm 0.5$  Ma; Paces and Miller 1993) was used as the standard.

### Analytical Results

**Radiometric Data.** We imaged and analyzed zircons from six samples from the Ireteba pluton. Almost all grains displayed distinct cores. Thick, pre-

sumably magmatic overgrowths are dark and unzoned in backscattered electron images, except for thin, euhedral, oscillatory-zoned rims (fig. 5). The thin rims are richer in U and yield concordant ages that straddle the Cretaceous-Paleogene boundary. Sixteen of 19 rim analyses fell in the range 60–69 Ma; three were much younger (26–52 Ma; figs. 6a, 7a). This is generally consistent with the results of extensive monazite Th-Pb dating by ion probe, which yielded a clear maximum for magmatic zones at 64 Ma (fig. 6b), another maximum

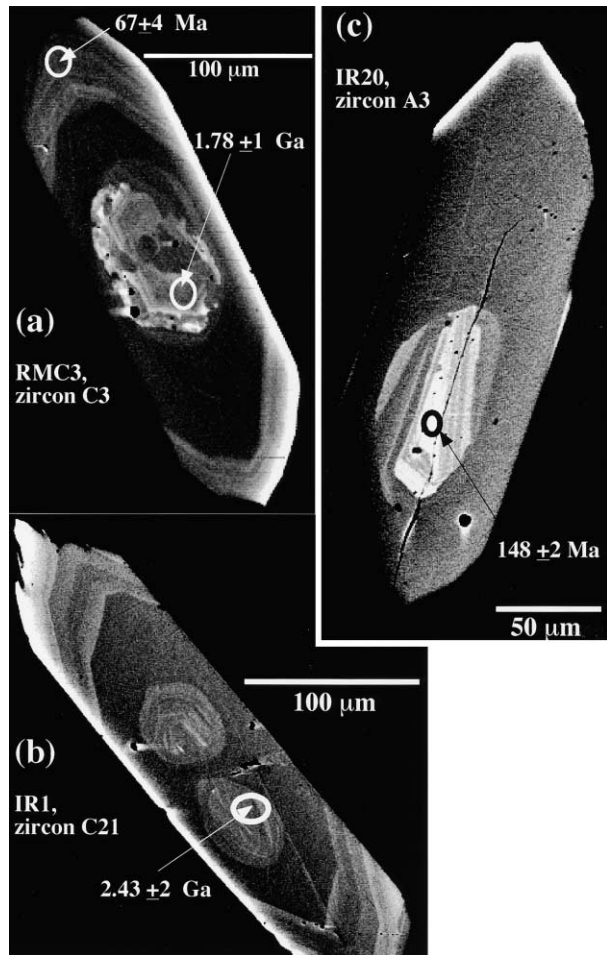


**Figure 5.** Backscattered electron images of representative zircons. Ellipses show sizes and locations of analytical spots. All analyses of illustrated points are concordant;  $^{206}\text{Pb}/^{238}\text{U}$  ages are given for Mesozoic ages,  $^{207}\text{Pb}/^{206}\text{Pb}$  for Proterozoic ages. Stated  $2\sigma$  errors are in the last decimal place.

at 16 Ma that reflects replacement during Miocene extension and magmatism, and fewer analyses of intermediate age that are interpreted to represent “mixed” points that straddled boundaries between zones of the two ages and possibly partial Pb loss (Townsend et al. 2000). The post-60 Ma zircon ages also probably are a result of Miocene processes that induced partial recrystallization and Pb loss. The remaining 16 ages yield a pooled weighted mean age of 64.5 Ma but with a very high MSWD of 8.9, indicating that they do not represent a single uniform population. By excluding those ages less than 64 Ma (i.e., those younger than the apparent monazite age and presumably partly reset), we calculate a pooled age of  $67.1 \pm 0.8$  Ma ( $2\sigma$ ; MSWD = 1.4,

$n = 10$ ). Also excluding the oldest age (69.4 Ma), which appears to be a statistical outlier, results in a pooled age of  $66.4 \pm 0.9$  Ma ( $2\sigma$ ; MSWD = 1.2). We interpret the true age to be between 64 and 69 Ma, that is,  $66.5 \pm 2.5$  Ma.

There are two distinct age populations of inherited cores, Early Proterozoic (15 of 19) and Jurassic (4; fig. 7b, 7c). Proterozoic core ages are dominantly 1.6–1.8 Ga, but three are between 2.0 and 2.4 Ga and one is concordant at 1.50 Ga. The Jurassic ages are 150–170 Ma.

**Major and Trace Element Geochemistry.** Ireteba granite is uniformly felsic and strongly peralumi-

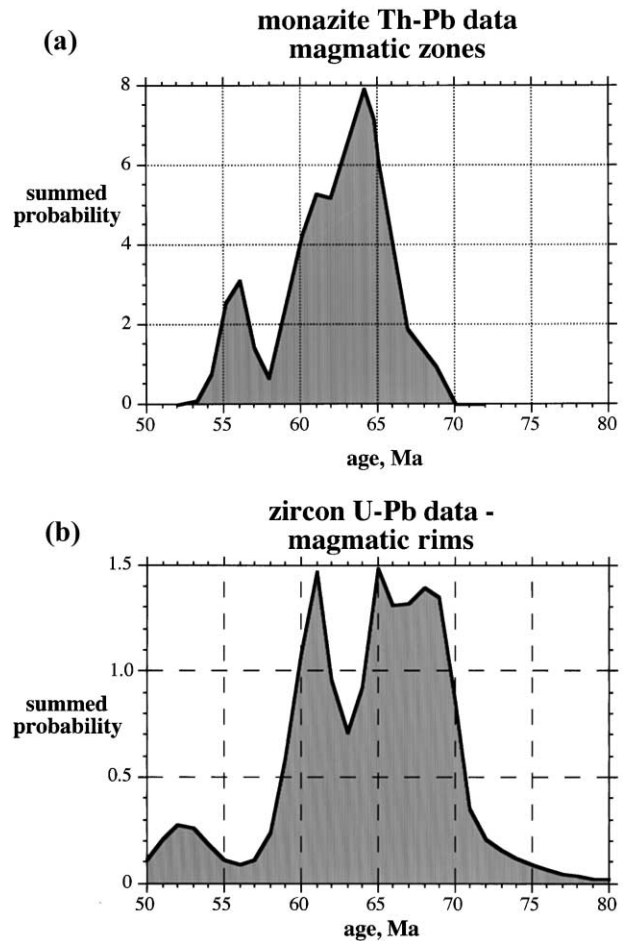


**Figure 6.** Probability plots of ion probe ages thought to reflect magmatic crystallization (post-50 Ma and pre-80 Ma portions of spectra omitted). Gaussian probability distributions of individual analyses are summed by million-year interval so that each analysis has an area of one with height proportional to precision (cf. Deino and Potts 1992). *a*,  $^{208}\text{Pb}/^{232}\text{Th}$  ages of zones in monazite interpreted to be magmatic (Townsend et al. 2000); *b*,  $^{206}\text{Pb}/^{238}\text{U}$  ages of zircon rims (this study).

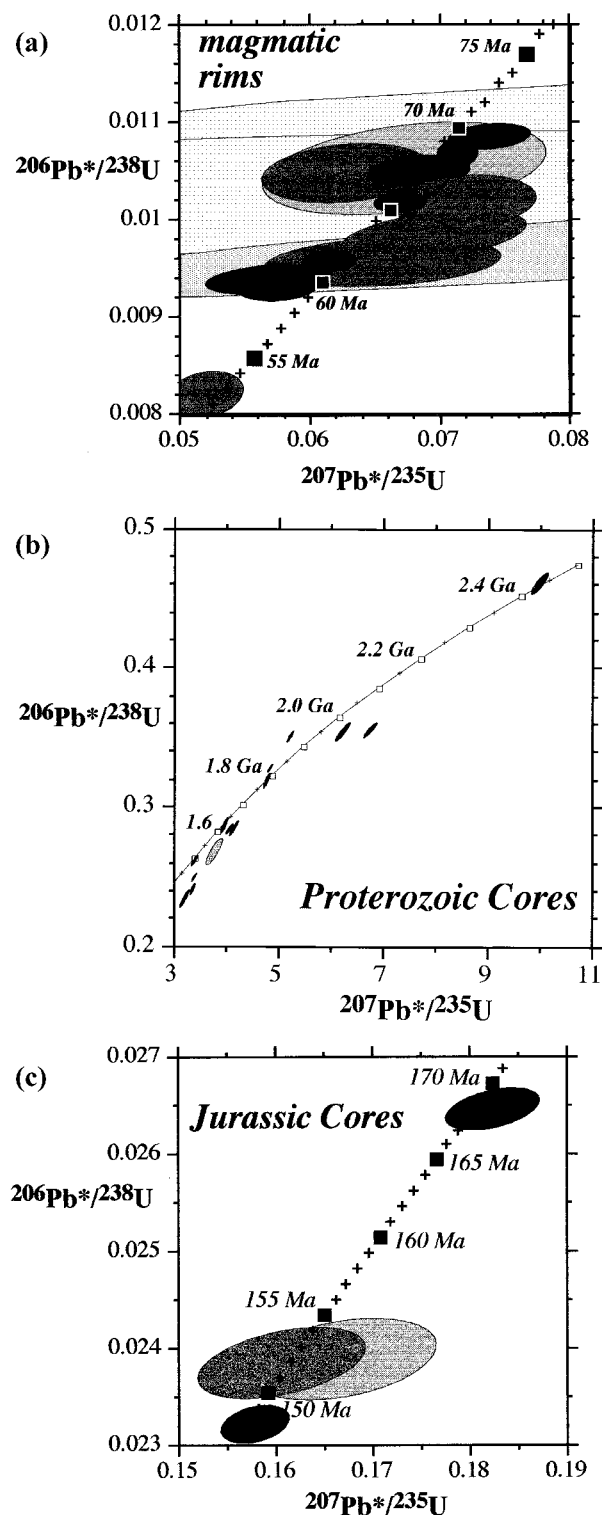


**Figure 7.**  $^{206}\text{Pb}/^{238}\text{U}$  versus  $^{207}\text{Pb}/^{235}\text{U}$  concordia plots of zircon analyses. Error ellipses are  $1\sigma$ ; darkness of shading of ellipses qualitatively indicates precision (smaller errors = darker ellipses). *a*, Magmatic rims; *b*, Proterozoic cores; *c*, Jurassic cores.

nous, with approximately 1%–2% normative corundum and silica ranging from 70 to 77 wt% (table 1). Major and trace element concentrations of the granites plot with generally consistent trends on variation diagrams, with compatible elements (Ca, Mg, Fe, Ti, Al, Sr, Ba, light rare earth elements [LREE]) decreasing and incompatible elements (Rb, K [though scattered]) increasing with increasing  $\text{SiO}_2$  (fig. 8). Strontium concentrations are notably high for felsic rocks (fig. 8*d*, 8*e*). With the exception of the most felsic sample analyzed, the granites have about 100 times chondritic LREE, are highly depleted in heavy rare earth elements (HREE;  $\sim 2$ –4 times chondrite), and lack Eu anomalies or have slight positive anomalies (fig. 9*a*).

Silica contents in the mafic to intermediate rocks range from 50 to 67 wt% (table 1). They also form fairly coherent element-element trends for some elements, but for others plots are highly scattered. They do not in general form well-defined trends when plotted with the granites, and in some diagrams inflections are evident at the transition from mafic to felsic (fig. 8). The mafic rocks have LREE concentrations as high as or higher than those of the granites and have more typical crustal HREE abundances ( $\sim 10$  times chondrite; fig. 9*b*).

**Isotope Geochemistry.** Initial  $^{87}\text{Sr}/^{86}\text{Sr}$  ratios of granite samples range from 0.712 to 0.716 and  $\epsilon_{\text{Nd}}$  from  $-15.3$  to  $-17.3$  (table 1; fig. 10). The mafic samples have initial  $^{87}\text{Sr}/^{86}\text{Sr}$  between 0.708 and 0.709 and  $\epsilon_{\text{Nd}}$  from  $-6$  to  $-8$  (table 1; fig. 10). The mafic rocks plot within the field of enriched mantle basalts from the Mojave region on initial  $^{87}\text{Sr}/^{86}\text{Sr}$  versus  $\epsilon_{\text{Nd}}$  plots, and the granites cluster at somewhat more primitive values than most of the Proterozoic crust of the Mojave terrane (Miller and Wooden 1994). Lead isotope ratios of Ireteba granite feldspar separates range from 17.78 to 18.04 ( $^{206}\text{Pb}/^{204}\text{Pb}$ ), 15.49 to 15.59 ( $^{207}\text{Pb}/^{204}\text{Pb}$ ), and 37.8 to 39.6 ( $^{208}\text{Pb}/^{204}\text{Pb}$ ). Ratios of two mafic rocks are slightly higher (18.12–18.18, 15.59–15.62, 39.1–39.5). These values span a range that extends from the field for Early Proterozoic rocks from the Mojave province to the field for the Arizona crustal province (table 1; fig. 11).

One granite and one mafic whole-rock sample each yielded a  $\delta^{18}\text{O}$  value of 5.4‰, probably reflecting interaction with high-temperature fluids. The other four analyzed samples, all granites, ranged from 8.2‰ to 8.8‰ (two of the analyzed samples are from Townsend et al. 2000). Quartz separates from two granites had  $\delta^{18}\text{O}$  values of 10.2‰ (table 1). The quartz data and the majority of the whole-rock data indicate that the granitic magma had  $\delta^{18}\text{O}$  of about 8.5‰, well within the range of normal

**Table 1.** Elemental and Isotopic Compositions of Samples

	Granite											
	FB3	FC2	I23	I31	I40	I51	I56	IE3	IE7	IKH2	IN1	IR20Z
Oxides (wt%): <sup>a</sup>												
SiO <sub>2</sub>	74.14	74.84	73.38	74.72	74.76	75.55	74.84	74.02	73.93	71.70	73.97	73.12
Al <sub>2</sub> O <sub>3</sub>	14.91	14.66	15.38	14.84	14.63	14.56	14.51	14.88	14.85	15.91	15.08	14.99
FeO (total)	.99	.71	.91	.79	.99	.60	1.21	.83	1.04	1.39	.77	1.13
MgO	.18	.14	.20	.18	.17	.12	.26	.23	.22	.31	.24	.38
MnO	.00	.02	.02	.00	.02	.05	.02	.01	.03	.02	.01	.03
CaO	1.37	1.56	1.38	1.04	1.16	.64	1.41	1.61	1.61	1.54	1.35	1.72
Na <sub>2</sub> O	3.84	4.11	4.26	4.13	4.01	4.41	4.15	4.31	4.56	4.61	4.34	4.86
K <sub>2</sub> O	4.43	3.88	4.26	4.11	4.06	3.91	3.36	3.89	3.52	4.24	4.02	3.48
TiO <sub>2</sub>	.09	.05	.13	.12	.14	.07	.16	.16	.18	.21	.16	.19
P <sub>2</sub> O <sub>5</sub>	.04	.03	.07	.07	.06	.08	.07	.05	.06	.07	.06	.08
LOI	1.05	.50	.60	.85	.70	.60	.55	.55	.55	.75	.65	.88
(Total)	(99.64)	(99.38)	(100.08)	(99.89)	(99.81)	(99.47)	(99.83)	(99.99)	(99.57)	(99.49)	(99.48)	(99.62)
Mg <sup>b</sup>	25	26	28	29	24	27	28	33	28	29	36	38
Elements (ppm):												
Rb	70	72	154	129	144	176	111	107	117	128	116	90
Sr	505	471	465	413	415	186	441	560	491	610	617	708
Ba	1700	1400	1200	1100	960	190	820	1000	920	1300	1100	1400
Zr	100	55	130	120	130	41	120	150	150	170	150	120
Hf			2.9								3.4	4.2
Y	4	25	16	6	13	23	32	16	8	10	20	
Nb	5	5	11	12	11	26	17	9	11	10	12	18
U			.9								.6	1.3
Th			6.4								6.8	8.8
La			24.7								32	39.4
Ce			46.6								60.6	70
Pr			5.2								6.9	
Nd			16.9								24.1	26
Sm			2.7								3.6	3.9
Eu			.89								1.12	.83
Gd			1.9								2.6	
Tb			.3								.4	.4
Dy			1.2								1.7	
Ho			.26								.35	
Er			.6								1	
Tm			.1								.1	
Yb			.6								.9	.9
Lu			.11								.12	.12
Ratios: <sup>c</sup>												
<sup>87</sup> Rb/ <sup>86</sup> Sr <sub>m</sub>		.4664	.9803				1.0071				.5236	
<sup>87</sup> Sr/ <sup>86</sup> Sr <sub>m</sub>		.71575	.71463				.714583				.712238	.713411
<sup>87</sup> Sr/ <sup>86</sup> Sr <sub>i</sub>		.71532	.71373				.71365				.71180	.71300
<sup>147</sup> Sm/ <sup>144</sup> Nd <sub>m</sub>		.1134	.0938				.1013				.0869	.0948
<sup>143</sup> Nd/ <sup>144</sup> Nd <sub>m</sub>		.511747	.511779				.511773				.511806	.511767
ε <sub>Nd<sub>i</sub></sub>		-16.69	-15.91				-16.08				-15.31	-16.14
T <sub>DM</sub> (Ma) <sup>d</sup>		1967	1604				1719				1478	1633
<sup>206</sup> Pb/ <sup>204</sup> Pb (feld)	18.037	18.010	17.946								17.784	17.952
<sup>207</sup> Pb/ <sup>204</sup> Pb (feld)	15.579	15.587	15.584								15.490	15.552
<sup>208</sup> Pb/ <sup>204</sup> Pb (feld)	39.561	39.584	39.335								37.840	39.173
δ <sup>18</sup> O (‰; wr)			8.4				8.5				5.4	
δ <sup>18</sup> O (‰; qtz)							10.2					

<sup>a</sup> Oxides are normalized to 100%. Total Fe calculated as FeO. LOI = loss on ignition. (Total) indicates total of all oxides in initial analysis (prior to normalization), LOI.

<sup>b</sup> Molar Mg/(Mg + Fe).

<sup>c</sup> m = measured ratio; i = initial ratios calculated at 65 Ma using measured isotopic or trace element ratios. (wr) = whole rock; (qtz) = quartz separate; (feld) = feldspar separate. Nd isotopic data are normalized to <sup>146</sup>Nd/<sup>144</sup>Nd = 0.7219 and referenced to LaJolla Nd with <sup>143</sup>Nd/<sup>144</sup>Nd = 0.511850 as measured at the University of North Carolina during the period of analysis. Total procedure blanks for Rb, Sr, Sm, and Nd were less than 100 pg.

<sup>d</sup> T<sub>DM</sub> is depleted mantle model age after DePaolo 1981.

crust but low compared to many strongly peraluminous granites.

### Genesis and Evolution of the Ireteba Granite Magma

**Effects of Local Interaction with Mafic Magma.** Extensive interaction between the mafic and granitic

magmas indicated by field relations suggests that they influenced each other thermally, mechanically, and possibly chemically. A closed system relationship involving fractional crystallization is ruled out by the liquid-liquid contacts indicated by field relations, the near absence of rocks of intermediate composition, the contrast in mineralogy, and especially the strong disparity between the iso-

Granite								Mafic-intermediate rocks					
IS3	IS4	IS6	IS8	IS8B	IS30	OC4	OC11B	ICM4	IS1A	IS1B	OC8	OC11A	OC11C
74.74	75.33	70.36	77.22	75.58	74.59	72.83	73.07	50.57	62.64	50.32	54.24	67.08	56.42
14.95	14.80	15.58	12.99	13.80	14.26	15.53	15.08	15.53	17.49	16.57	20.17	19.09	15.78
.73	.43	2.83	.41	.78	.99	.84	1.01	9.56	4.48	9.47	7.07	1.39	10.26
.08	.06	1.27	.01	.17	.19	.12	.22	8.71	1.69	5.90	3.20	.65	3.68
.07	.05	.05	.00	.00	.07	.00	.01	.16	.05	.20	.08	.03	.16
1.24	1.16	2.57	.95	1.16	1.13	1.15	1.68	9.43	4.22	9.77	8.62	3.27	6.02
4.46	4.50	3.74	3.44	4.14	4.18	4.21	4.40	3.03	4.04	3.72	4.08	6.60	3.38
3.66	3.62	3.04	4.92	4.26	4.42	5.13	4.35	1.20	4.21	1.67	1.05	1.65	1.35
.04	.03	.40	.05	.09	.12	.12	.12	1.36	.88	1.74	1.21	.17	2.30
.03	.03	.16	.00	.03	.04	.06	.04	.45	.31	.65	.28	.06	.64
.50	.55	.45	.45	.45	.60	.50	.60	1.05	1.15	2.00	.90	.60	.50
(99.51)	(99.85)	(99.66)	(98.99)	(99.03)	(98.06)	(99.64)	(98.72)	(98.94)	(98.38)	(97.98)	(98.06)	(98.54)	(98.70)
17	20	45	4	29	26	21	29	62	40	53	45	46	39
122	115	72	101	80	119	94	89	24	84	50	26	41	50
338	333	722	279	346	268	379	490	740	858	763	1210	551	785
850	800	1400	680	1100	690	1000	1000	750	3000	620	660	340	520
78	97	150	86	95	52	120	80	170	380	240	130	120	91
	1.4	4.8							10	5.6	3.5		
18	13	14	6	21	26	7	25	35	33	30	16	24	30
7	9	8	4	4	8	9	4	12	19	17	6	10	15
	.3	.7							1.9	1.4	.5		
	2.5	7.7							8.8	6.2	3.1		
	12.7	29.5							71.6	62.4	23.1		
	25.9	55.6							150	132	46		
	3.2	6.3							18	16	5.6		
	11.5	19.5							63.7	62	22.3		
	2.6	3.2							9.4	10.7	4		
	.65	.7							2.93	2.79	1.42		
	2.2	2.8							7.1	8.5	3.4		
	.4	.4							1	1.2	.5		
	2.3	2.3							4.7	4.9	2.3		
	.51	.48							1	1.08	.46		
	1.3	1.3							2.6	2.5	1.2		
	.2	.2							.4	.3	.2		
	1.3	1.2							2.7	2.2	1.1		
	.19	.17							.39	.32	.15		
	.9923			.7193			.5349	.3411	.2874	.2021	.1138	.2432	.1957
	.716689			.715013			.71646	.706531	.708488	.708979	.709336	.715162	.70966
	.71577			.71435			.71565	.70622	.70822	.70879	.70923	.71494	.70948
	.1352			.0996			.0994	.1101	.0489	.1068	.1149	.1073	
	.511728			.511790			.511753	.512315	.512162	.512292	.512970	.511777	
	-17.25			-15.73			-16.46	-5.59	-8.06	-6.00	-7.93	-16.06	
2569				1670				1073	821	1073	1303	1812	
	18.036			18.176			18.020				18.186		18.119
	15.585			15.589			15.571				15.592		15.618
	39.580			39.388			39.512				39.138		39.538
										5.4			

topic compositions of the granitic and mafic rocks. Intimate mutual injection of the magmas suggests that mixing of mafic and felsic magmas might be responsible for isotopic and elemental variability of the granites. Local hybrid zones seem to support this possibility. However, rocks that appear to be hybrids are rare within the pluton, and there is a large gap in isotopic compositions between mafic rocks and granites, suggesting that mixing within the exposed pluton was not effective.

The Ireteba granite may have been influenced somewhat by its interaction with mafic magma, but major and trace element compositions of the mafic rocks and the granites do not form linear

mixing arrays (fig. 8). Furthermore, mixing of exposed granite and mafic rocks cannot explain the isotopic variability of the pluton as indicated by the models in figure 12. The characteristics of the Ireteba granitic magma were therefore established before its emplacement, and in the following sections we attempt to evaluate its genesis in terms of processes that occurred at deeper levels. We note, however, that the above lines of evidence do not preclude a role for mixing with mafic magma at depth.

**Petrogenetic Constraints: Introduction.** Distinctive geochemical and petrographic characteristics of the Ireteba granite place important constraints

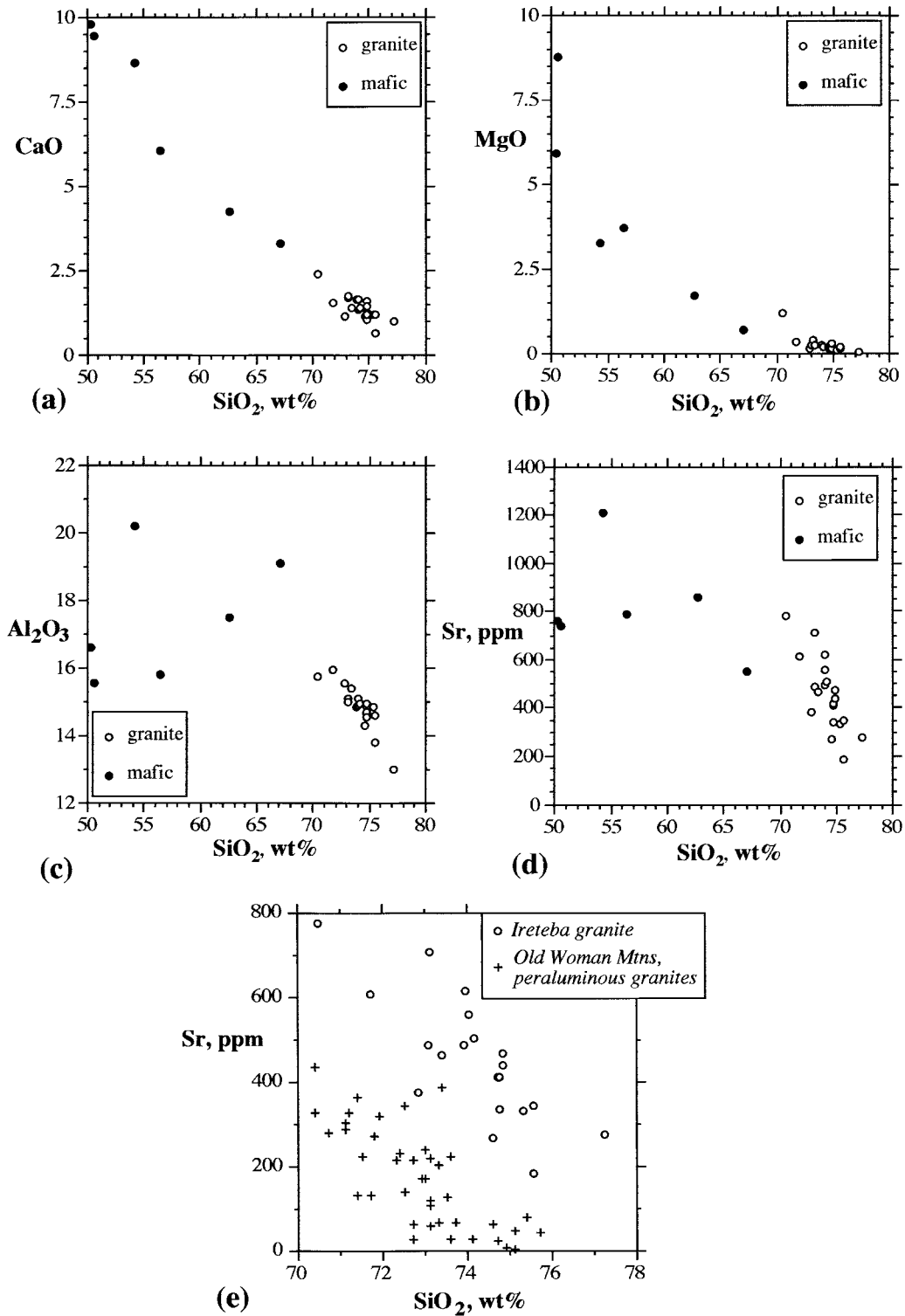


**Figure 8.** Variation of selected elements versus SiO<sub>2</sub>. a, CaO; b, MgO; c, Al<sub>2</sub>O<sub>3</sub>; d, Sr; e, Sr versus SiO<sub>2</sub> in Ireteba granites compared with peraluminous Cretaceous granites of the Old Woman Mountains, eastern Mojave Desert.

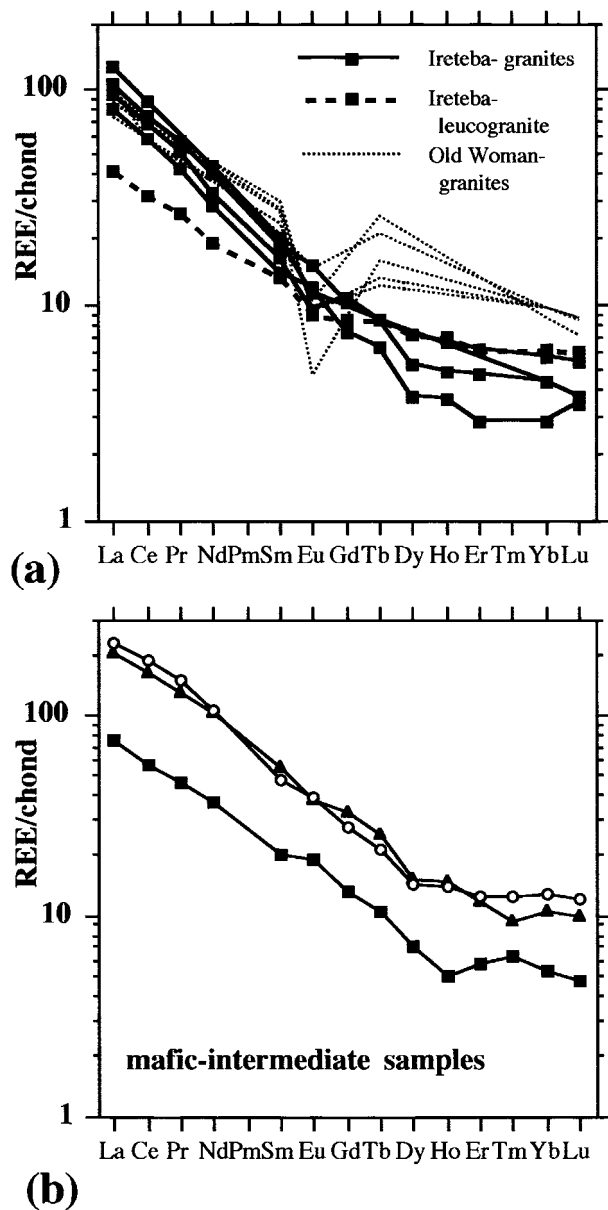


**Figure 9.** Chondrite-normalized rare earth element patterns. *a*, Ireteba granites; a more fractionated leucogranite is distinguished, and peraluminous granites of the Old Woman Mountains are shown for comparison. *b*, Mafic to intermediate rocks.

on its genesis. First, Sr, Nd, and Pb isotopic compositions and Proterozoic zircon inheritance indicate that it is primarily derived from ancient crust. Second, high Sr concentrations, absence of a negative Europium anomaly, straight rare earth element (REE) patterns (i.e., no middle REE depletion), and strong HREE depletion indicate a relatively feldspar-poor, garnet-rich source. Finally, the abun-

dant, large quartz crystals present throughout the pluton suggest that quartz may have been present early in the history of the magma and possibly in the residue of melting. We discuss these constraints in detail in the following sections.

**Trace Element Constraints: Deep Crustal Residues.**

We have tested the constraints imposed by the distinctive trace element chemistry of Ireteba granite by constructing simple inverse models that assume (1) the Ireteba granite magma was generated by crustal anatexis and (2) the average granite composition is an adequate approximation of the primary melt composition. While neither of these assumptions is likely to be strictly correct, deviations are unlikely to affect our conclusions. Isotopic compositions suggest the possibility of mantle input, but it probably was small (see section on isotopic constraints) and it could not have imparted the characteristic Ireteba trace element signature. We doubt that the magma fractionated much before emplacement—if it had, feldspar extraction would have resulted in lower Sr and Eu concentrations.

The following trace element characteristics provide especially strong constraints on petrogenesis. (1) The granite has less than half the HREE content of typical mafic to felsic igneous rocks and potential crustal sources in general. This indicates that

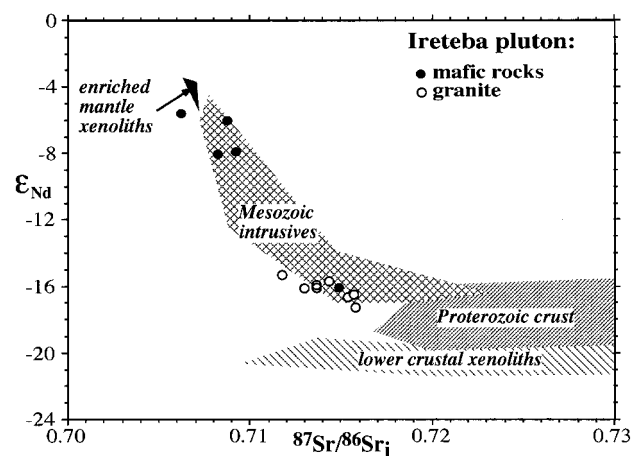


**Figure 10.** Initial Sr-Nd isotopic compositions of Ireteba samples compared with coeval compositions of regionally significant lithologies of the eastern Mojave terrane and nearby areas. Proterozoic crust of the eastern Mojave Desert (Miller and Wooden 1994); lower crustal xenoliths (Hanchar et al. 1994); Mesozoic granitoids (Miller and Wooden 1994; Allen et al. 1995); enriched mantle xenoliths in Cenozoic basalts (Beard and Glazner 1995; Mukasa and Wilshire 1997). “Mafic” data point that plots with granites (sample OC11A) appears in the field to be a hybrid but has 67 wt% SiO<sub>2</sub>.

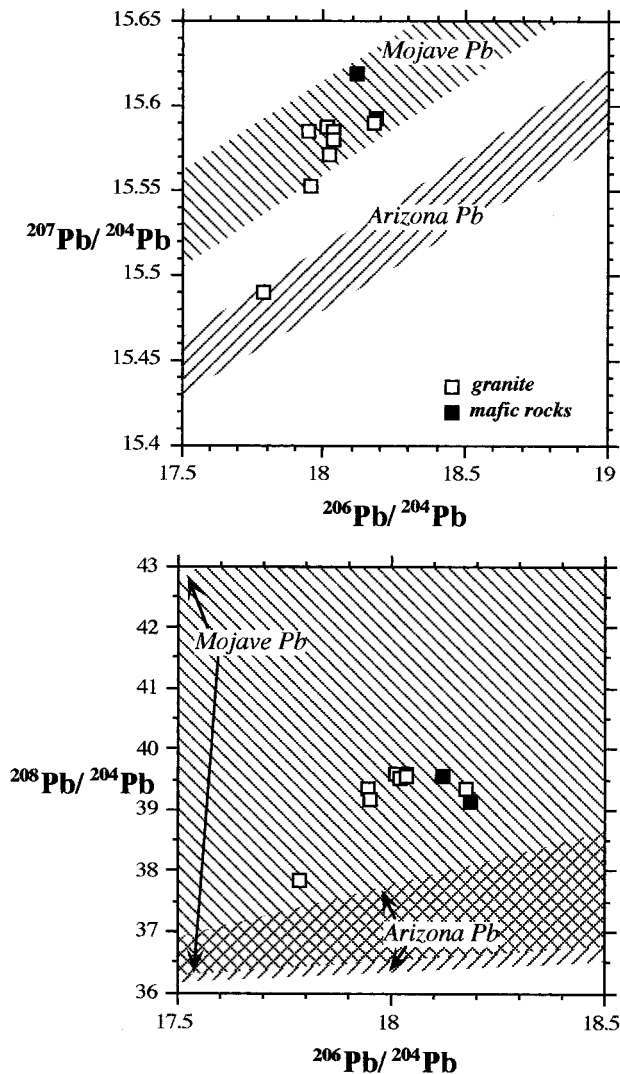


**Figure 11.** Pb isotopic compositions of Ireteba samples compared with fields of Arizona and Mojave terranes (Wooden et al. 1988).

HREE were strongly enriched in the residue of melting. (2) REE patterns are straight, lacking the inflection at the LREE-to-HREE transition common in igneous rocks. Lack of relative depletion in middle REE suggests that phases that concentrate these elements did not dominate the residue. (3) Eu anomalies are generally absent and in some cases are positive. This implies that minerals that strongly fractionate Eu from the other REE were either absent in the residue or that minerals with balancing positive and negative Eu partition coefficient anomalies were present (given that much of the fertile crust has a negative anomaly, dominance of residual minerals that preferentially reject Eu is

also possible). (4) Sr and Ba concentrations are higher than those of average crust. Rocks that match or exceed Ireteba endowment of both elements are limited to alkalic and some intermediate rocks (high-K calc alkalic dacites, quartz latites, granodiorites, quartz monzonites). This characteristic appears to require that the residue was poor in minerals that concentrate Sr and Ba.

Constraint 1 suggests the presence of garnet and/or hornblende, the only potentially abundant crustal minerals with high  $K_D$ 's for HREE, in the residue. Constraint 2 indicates that hornblende alone is not likely to have been responsible for HREE depletion because it has higher  $K_D$  for middle REE (MREE) than for HREE. Constraint 4 indicates that plagioclase, K-feldspar, and micas were not abundant in the residue because they would concentrate Sr and/or Ba and leave the melt depleted in these elements. Constraint 3 also argues against the presence of abundant feldspar, though garnet

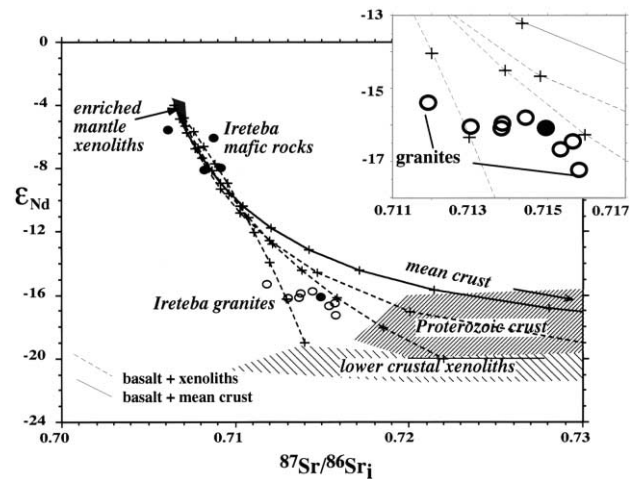


**Figure 12.** Initial Sr-Nd isotopic compositions of Ireteba samples compared with simple bulk mixing models. The mafic end member is taken to be a hypothetical basalt ( $\epsilon_{Nd} -4$ , 40 ppm Nd,  $^{87}Sr/^{86}Sr$  0.7065, 1000 ppm Sr) derived from enriched lithospheric mantle similar to the xenoliths of figure 10 (Beard and Glazner 1995; Mukasa and Wilshire 1997); this basalt is consistent with the compositions of presumed lithosphere-derived mafic magmas from this region (see, e.g., Farmer et al. 1989; Daley and DePaolo 1992; Metcalf et al. 1995; Bachl et al. 2001). Crustal end members are mean eastern Mojave Proterozoic crust of the nearby Old Woman Mountains region ( $\epsilon_{Nd} -18$ , 50 ppm Nd,  $^{87}Sr/^{86}Sr$  0.74, 200 ppm Sr; Miller and Wooden 1994) and selected deep crustal xenoliths (Hanchar et al. 1994). Inset emphasizes distribution of granite compositions with respect to model mixing curves.

and hornblende have negative Eu  $K_D$  anomalies and thus can offset the effect of feldspar.

In addition, trace element modeling reveals the following constraints. (5) Using melt fractions less than ~50%–70% and source compositions modeled as combinations of Ireteba granite and a residue consisting of major crustal phases, LREE are unrealistically low. We infer that the residue contained an LREE-rich accessory phase, probably monazite, and that the LREE concentration of the melt was therefore governed by solubility and not by Henry's Law partitioning. Therefore, we exclude the LREE from our trace element models. (6) Unless melt fraction was unrealistically high (granite ~ source composition), the total fraction of hornblende + garnet + mica + feldspar in the residue is limited (hornblende and garnet can deplete the melt too much in MREE and HREE; see constraints 3 and 4 regarding micas and feldspar). This implies that diluting phases with lower  $K_D$ 's for the modeled trace elements were relatively abundant (probably at least 40% of the residue). Other phases that could remain in the residue of crustal anatexis include quartz and pyroxenes. Its occurrence as resorbed megacrysts and the high silica concentration of the granite support quartz as a residual phase; the presence of pyroxene remains speculative and would require relatively high-temperature melt generation. Aluminous phases (sillimanite, cordierite) are unlikely to have been abundant, because this would require a dominantly pelitic source, which is precluded by the low  $\delta^{18}\text{O}$  and high Na and Ca of the granite.

Figure 13 illustrates some of the constraints imposed by trace element modeling. Figure 13a compares average Ireteba granite to average upper crust (the normalization factor), average crust, and the North American shale composite (NASC; Taylor and McLennan 1981; Gromet et al. 1984). Rocks of the Early Proterozoic Mojave terrane crust, which constitute the majority of exposed regional crust, have concentrations of these elements similar to NASC, whereas post-1.7 Ga Proterozoic rocks are richer in Ba and REE, and Mesozoic granitoids are similar to Ireteba granite in Ba and Sr but otherwise like "normal" crust (Miller and Wooden 1994). Figure 13b illustrates two reasonable model residues. Each contains garnet plus small amounts of biotite and plagioclase and a large amount of diluting phases (in this case quartz and orthopyroxene were used); one of the models includes hornblende. "Success" of these model residues means that they can be combined with Ireteba granite to yield an original source composition that is reasonably similar to typical crustal materials like the simplified av-

erages in figure 13a (see also Taylor and McLennan 1981; Rollinson 1993). Figure 13c shows examples of failed models that include too much hornblende, plagioclase, or biotite, resulting in unrealistic concentrations of middle REE, Sr and Eu, and Ba, respectively. More than ~15% K-feldspar will also result in too high Sr and Ba. More details of the modeling can be found in D'Andrea (1998) or may be obtained from the authors.

We conclude that the Ireteba magma left a garnet-bearing residue that was very poor in feldspar (compared to typical crust) and had a limited amount of (or no) hornblende and biotite. Additional phases with low  $K_D$  for Rb, Sr, Ba, and REE, probably including quartz, were abundant in the residue, and monazite or another LREE mineral was present. This assemblage suggests that melting took place deep in the crust, where garnet is stabilized, quartz solubility in melt diminishes, and feldspar solubility increases (see following section).

**Phase Equilibria Constraints: Melt Production in the Deep Crust.** We conclude that the Ireteba granite represents a primarily crustal melt; therefore, the phase equilibria of crustal melting can be used to constrain its petrogenesis. Experimental data reveal that plagioclase  $\pm$  K-feldspar is abundant in the melt residues of all crustal lithologies that yield granitic melts, except under high-pressure and/or high-temperature conditions (Patiño Douce and Beard 1996). Experiments that involve melting of a variety of crustal materials at deep crustal pressures (~10 or more kbar, 800°–900°C) demonstrate that strongly peraluminous melts are produced with garnet-bearing, quartz-rich, plagioclase-poor residues (LeBreton and Thompson 1988; Vielzeuf and Montel 1994; Gardien et al. 1995; Patiño Douce 1995; Patiño Douce and Beard 1995, 1996). In most cases, extensive crustal melting is thought to be triggered by biotite dehydration at temperatures in excess of 800°C (Gardien et al. 1995; Patiño Douce and Beard 1995). McCarthy and Patiño Douce (1997) also showed that high-temperature (>900°C) peraluminous felsic melts and a garnet-rich residue can be produced by basaltic injection and hybridization of the deep crust (see also Patiño Douce 1999).

Zircon and monazite saturation thermometry (Watson and Harrison 1983; Rapp et al. 1987) suggests further constraints on generation of the Ireteba magma. The facts that zircons contain abundant inherited cores and that monazite was an early crystallizing phase suggest that the Ireteba melt was saturated in both minerals at or near its source and throughout subsequent crystallization. Assuming the granites represent melt compositions, the

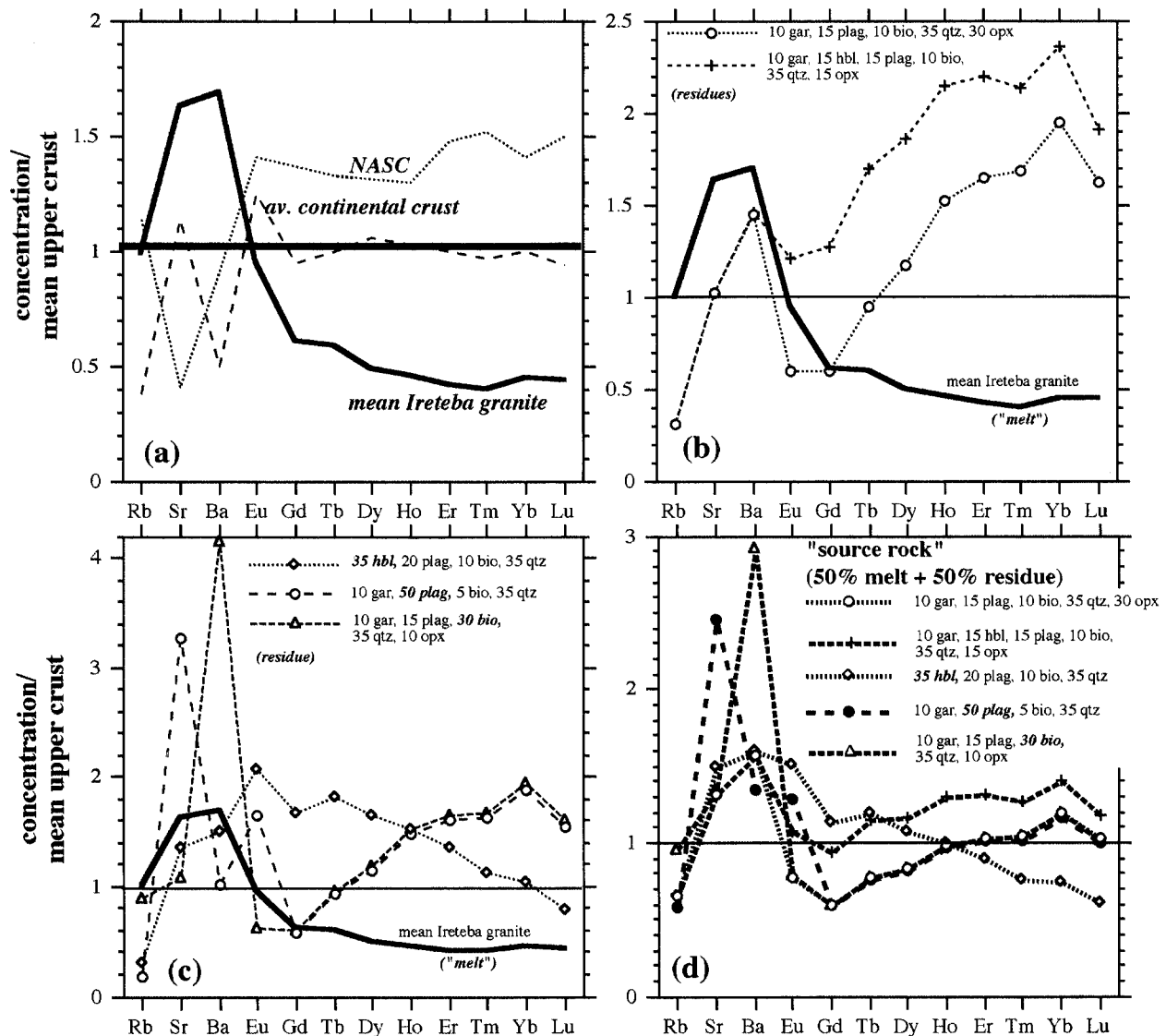


**Figure 13.** Trace element modeling of petrogenesis of Ireteba granite. All trace element concentrations normalized to "present average upper continental crust" of Taylor and McLennan (1981). Models were calculated assuming that average Ireteba granite approximates melt extracted from the source; trace element concentrations in residues in equilibrium with this "melt" were calculated using  $K_D$ 's from Rollinson (1993). *a*, Ireteba granite compared to present-day average upper continental crust (normalization), North American shale composite (NASC; Haskin et al. 1968; Gromet et al. 1984) and present-day average crust (Taylor and McLennan 1981). *b*, Examples of "successful" models: combinations of residue with reasonable "melt" fractions have compositional patterns that are similar to normal crustal rocks. *c*, Examples of "unsuccessful" models demonstrating that abundant hornblende, plagioclase, or biotite in the residue yield unrealistically high concentrations of middle REE, Sr and Eu, and Ba, respectively. *d*, Model compositions of "sources" assuming 50% melting; each pattern represents a 50/50 mixture of Ireteba granite as "melt" and a specified residue in equilibrium with the Ireteba melt.

21 analyzed samples yield zircon saturation temperatures ranging from 692° to 794°C, with the lowest  $T$  for a highly fractionated aplite dike and the highest for a probable cumulate-rich rock. The apparent zircon saturation  $T$  for the mean of Ireteba granites is 761°C. The monazite saturation tem-

peratures for the five granites for which we have REE data range from 709° to 771°C, with a value for mean granite of 760°C. If the magmas were in fact saturated in zircon and monazite at the source, as we have argued, ~760°C is a good approximation of the temperature of magma generation. (Although

plutonic rocks are not simply solidified liquids and magma compositions are modified during ascent, it is unlikely that the granite was strongly fractionated between source and emplacement because fractionation would have resulted in depletion in Sr and development of a negative Eu anomaly. The small fraction of undissolved, inherited zircon [ $<10\%$ , based on estimated volume proportions of cores from images; cf. fig. 5] has minimal effect. Solubilities of zircon [and monazite] are extremely sensitive to temperature; an overestimate of Zr concentration in melt of 10% would result in overestimation of  $T$  by less than  $10^\circ\text{C}$ . Likewise, the discrepancy between major element compositions of granitic rocks and coexisting granitic melts is not enough to affect temperature estimates appreciably. Therefore, the mean composition of the pluton should provide an adequate estimate of initial melt composition.)

The relatively low estimated temperature for the Ireteba magma is below that of incipient biotite dehydration at moderate to high pressure (slightly in excess of  $800^\circ\text{C}$ ; see references above) and well below that of the hybridized melts of McCarthy and Patiño Douce (1997). This implies one of the following: (1) Our temperature estimate is too low by  $\sim 50^\circ\text{C}$  or more. It is possible that the calibration for zircon thermometry permits errors of this magnitude, but the method appears to yield good results where it can be tested (Miller and Meschter 2000). The assumption that mean Ireteba granite is an adequate approximation of initial melt composition could also be faulty. However, extreme fractionation of zircon would be required to drop Zr concentration enough to yield a  $50^\circ\text{C}$  lower calibrated  $T$ . It is also possible that the melt was not initially saturated in zircon—that the inherited grains were preserved either as inclusions in other grains or as metastable remnants whose survival resulted from slow dissolution rates (Watson 1996). In most cases, dissolution is probably fast enough to prevent metastable preservation throughout the entire process of melting, segregation, ascent, and solidification. However, zircons might survive a very rapid heat pulse accompanying crustal melting and hybridization by mafic magma (McCarthy and Patiño Douce 1997) if the resulting melt quickly cooled to temperatures at which it could achieve true saturation. Or (2) generation of melt by biotite dehydration or mafic magma/crust hybridization can take place at lower  $T$  than previously estimated. This is plausible, but we know of no evidence to support it. Or (3) another melting mechanism was involved. The saturation temperatures are consistent with muscovite dehydration melting (cf. Pa-

tiño Douce and Harris 1998). However, this mechanism yields a melt fraction only equivalent to the fraction of muscovite that breaks down; hence a very muscovite-rich source is required to generate appreciable melt. Such sources require a pelitic protolith, which is ruled out as a principal source material. Alternatively, addition of several percent water to a more quartzofeldspathic source at  $T = 750^\circ\text{--}800^\circ\text{C}$  would induce a sizable melt fraction.

Regardless of the mechanism of melting, a combination of trace element evidence and constraints of phase equilibria suggests that the granitic magma was extracted from a deep crustal residue that contained garnet and quartz, was not mica rich, and contained considerably less feldspar than the 50+ % that characterizes the crust. It is likely that this crust was heterogeneous and plausible that it was hybridized by mafic magma (Miller et al. 1988; Patiño Douce 1999).

**Isotopic Constraints: Ancient Crust, Juvenile Contribution.** Initial  $^{87}\text{Sr}/^{86}\text{Sr}$  and  $\epsilon_{\text{Nd}}$  of the granites, though highly evolved compared with possible mantle sources, cluster at more primitive values than most of the known Proterozoic crust of the Mojave region. This indicates a strong crustal component involved in their generation but suggests the possibility of involvement of a more juvenile component. In detail, the granites define a trend that suggests mixing.

Representative mixing models using mafic and felsic end members appropriate for the regional crust are presented in figure 12 (see D'Andrea 1998 for more models, including the synplutonic mafic dikes and the most evolved granite as end members; results are essentially the same). The granite array generally had lower  $\epsilon_{\text{Nd}}$  for a given  $^{87}\text{Sr}/^{86}\text{Sr}$  than the model mixing curves. To account for this discrepancy, either the mixing curve must be more strongly concave upward (i.e., lower  $[\text{Nd}/\text{Sr}]_{\text{mafic}}/[\text{Nd}/\text{Sr}]_{\text{felsic}}$  than modeled end members) or one or both end members must have lower  $\epsilon_{\text{Nd}}$  and/or lower  $^{87}\text{Sr}/^{86}\text{Sr}$ . Lower crustal xenoliths from the nearby Mojave Desert (Hanchar et al. 1994) yield more satisfying results. Although mixing between typical enriched basalts and individual xenoliths cannot reproduce the granite array, the swath of mixing curves generated by the xenoliths + enriched basalt encompasses the range of granite compositions. All plausible models suggest that the granites are primarily crustally derived but probably have  $\sim 10\%$ – $25\%$  juvenile component.

**Mechanisms of Hybridization.** Field evidence, geochemical data, and the constraints from isotopic and trace element modeling indicate that the Ireteba granite was generated in the deep crust pri-

marily from Proterozoic crustal material but with a significant mantle component. The hybridization reflects a deep-level process. A major question in this general model is when and how the ancient crust interacted with juvenile mafic magma. We envision three general possibilities. (1) The crust may have been modified during the Proterozoic—amphibolite and mafic gneisses are fairly common in the Mojave terrane—and remained unmodified until the onset of melting to form the Ireteba granite. (2) Hybridization may have occurred earlier in the Mesozoic as a result of mantle input during regional magmatism. (3) Mafic magmas associated with those that formed the synplutonic dikes may have produced a hybrid zone in the deep crust that directly yielded the Ireteba granite. Although it would be difficult to disprove, we see no direct evidence that supports possibility 1. However, the inherited Jurassic cores in Ireteba zircons support possibility 2 and the synplutonic dikes themselves lend credence to 3, and so our preferred interpretation is that either 2 or 3, or both, was involved in granite genesis. Whether or not the synplutonic mafic magma contributed directly to hybridization, we consider it likely that it played an important role in magma generation as a heat source.

### Discussion

**Significance of Mafic Magma Interaction in Petrogenesis of Peraluminous Granites.** Field relations clearly document interaction between mafic and strongly peraluminous magmas in the Ireteba pluton. Such interaction has not been widely reported in peraluminous plutons. The common perception that peraluminous granites are wholly crustally derived and the widespread observation that fine-grained mafic enclaves are vastly more common in weakly peraluminous and metaluminous granitoids than in peraluminous granites suggest that mafic/peraluminous interactions are rare and accidental or nonexistent. In recent years, a few examples of mafic magma/peraluminous granite mingling have been reported (see, e.g., Foster and Hyndman 1990 [Idaho batholith]; Clarke et al. 1997 [Nova Scotia]), and mafic enclaves and disequilibrium textures and assemblages interpreted to indicate mingling and/or mixing have been described (DiVincenzo et al. 1996; Elburg 1996a, 1996b, 1996c; Kontak and Clark 1997; Silva et al. 2000). Like the Ireteba granite, these other examples demonstrate little or no evidence for in situ magma mixing but display geochemical hints of hybridization of some sort during the evolution of the fel-

sic magmas. Patiño Douce (1999) suggests that a major global class of granitoids (Cordilleran peraluminous granites, named for the general habitat of the Ireteba pluton) were generated through interaction between basalt and graywacke-like material in the deep crust; in most cases, the direct evidence for this interaction is left behind at depth. Whether or not mafic magma contributed chemically to the Ireteba granite, such magma at least provided heat to the source region to induce melting. Even though there was abundant mafic magma in the deep part of the pluton, there is no direct evidence for its presence at higher levels—mafic enclaves are entirely absent. This may reflect properties (viscosity, density, temperature) and dynamic processes within felsic, strongly peraluminous magmas that obstruct the upward transport of mafic material and thus obscure its role in such magma systems.

**Regional Implications.** The Ireteba granite is one of many emplaced during Mesozoic through early Tertiary plutonism in the Cordilleran Interior (Miller and Bradfish 1980; Miller and Barton 1990). This magmatism is generally attributed to plate convergence, although whether it was entirely ocean-continent subduction or included a response to continent-continent oblique collision (Baja British Columbia; Maxson and Tikoff 1996) is uncertain. The Ireteba pluton differs from typical peraluminous granites in its high Sr and low HREE concentrations (figs. 8e, 9a) and extensive interaction with mafic magmas, and it apparently represents the last stage of magmatism at this latitude.

A few other peraluminous granites in the Colorado River region of southern Nevada and adjacent Arizona and California (Anderson and Cullers 1990; John and Mukasa 1990; John and Wooden 1990; see fig. 2) and elsewhere in the Cordilleran Interior (fig. 1; Ruby Mountains, northeastern Nevada [Lee et al. 1997]; Idaho Batholith [Schuster and Bickford 1985; Foster and Hyndman 1990; Foster and Fanning 1997]) share these geochemical characteristics. All appear to have been emplaced late in arc history. Most noteworthy is the enormous Bitterroot lobe of the Idaho batholith, in which synplutonic mafic dikes are common; to our knowledge, evidence for mingling has not yet been reported in any of the smaller plutons. Using the Idaho batholith as a model, Patiño Douce (1999) suggests that “Cordilleran peraluminous granites” share a hybridized, deep crustal source zone, but we note that the high-Sr, low-HREE composition seems to characterize only the youngest of Cordilleran Interior granites. The deep source plutons may constitute a late belt of distinctive magmas that mark a significant transition in tectonomag-

matic style at the local termination of convergence-related magmatism. At this time both a transition to extension in the upper crust (Hodges and Walker 1992) and flattening of subduction (Dumitru 1990) have been proposed. Either of these changes might be expected to bring about modification of the character of magmatism, but it is not obvious that either would induce both basaltic magmatism and deepening of the zone of crustal anatexis.

**Deep-Source Granitoids: Petrogenetic and Tectonic Affinities.** We interpret the Ireteba granite to have been generated at relatively great depth, at least 35–40 km. The principal evidence for this conclusion lies in the high Sr and Eu concentrations and low HREE, which together suggest paucity of feldspar and presence of garnet in the crystalline residue. These same trace element characteristics have been noted in voluminous Archean trondhjemite-tonalite-granodiorite (TTG) intrusions that make up a major part of the early crust (Jahn et al. 1981; Martin 1986, 1999) and in Phanerozoic volcanic and plutonic rocks loosely referred to as adakites (fig. 14; Defant and Drummond 1990; Drummond and Defant 1990; Defant and Kepezhinskis 2001). Recognition of the distinctive high-Sr and high-Eu, low-HREE signature in Phanerozoic rocks and of its depth significance has increased dramatically in the last decade.

Most petrogenetic-petrotectonic interpretations have centered on mafic sources in convergent environments—either metabasalt in a subducting slab (hence adakite; Defant and Drummond 1990) or mafic rock in thickened crust (e.g., underthrust arc crust; Muir et al. 1995; Miller et al. 1997). Although this “deep signature” in Phanerozoic rocks is generally considered in isolation, references compiled by Drummond and Defant (1990), in addition to more recent studies, demonstrate that it is not rare. Furthermore, the current study and others demonstrate that, contrary to earlier assumptions, this signature is not restricted to low-K rocks (trondhjemites and tonalites) that were derived from isotopically primitive sources. The Bitterroot lobe of the Idaho batholith, like the Ireteba granite, has high Sr and Eu and low HREE, together with highly evolved Nd and Sr isotopic compositions and abundant zircon cores that indicate a dominant ancient crustal component (Schuster and Bickford 1985). We suggest that “adakite” characteristics by themselves are simply a deep-source signature that indicates melting of crustal material at great depth. Neither a subducting slab nor a mafic source is required. Where subduction is unlikely or untenable, the depth of the source requires a thickened

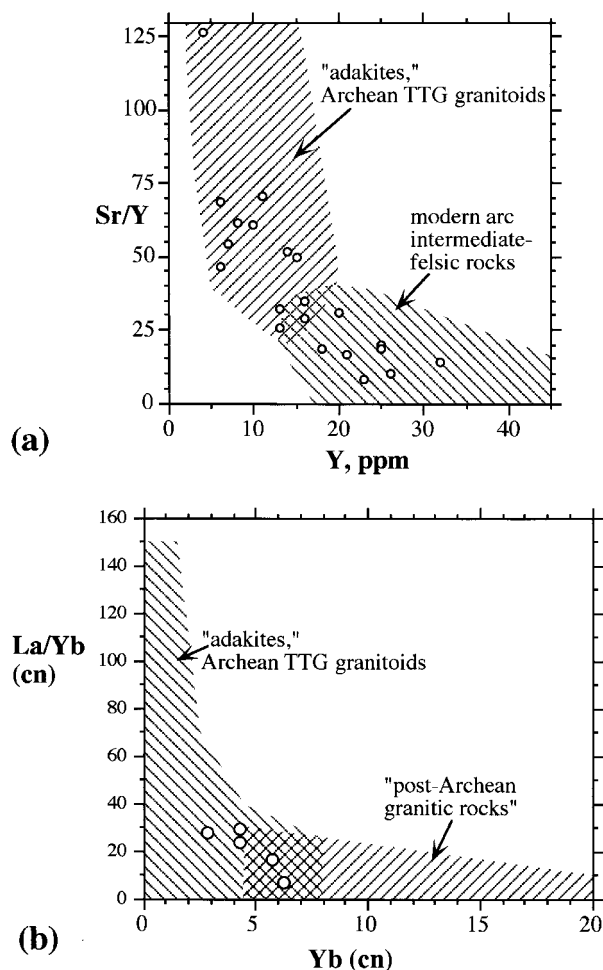


**Figure 14.** Ireteba granites compared with “adakites” and modern arc and granitic rocks (Defant and Drummond 1990; Drummond and Defant 1990; Defant et al. 1991; Yogodzinski et al. 1995). *a*, Sr/Y versus Y concentrations; *b*, chondrite-normalized La/Yb versus Yb.

crust, and preservation of the deep-source signature suggests limited fractionation in the upper crust.

### Conclusions

The strongly peraluminous Ireteba Granite was generated late in the arc history of the Cordilleran Interior of the western United States and documents extensive interaction with mafic magmas. Its source was dominantly ancient crust, as is clearly documented by its isotopic composition and the abundance of inherited zircon. However, a more juvenile component was also important. This component could be represented by either the observed mafic igneous rocks of the Ireteba pluton or the Jurassic zircon cores that document the presence

of underlying Mesozoic igneous rocks. Melting occurred deep in the crust, as suggested by the low HREE concentrations (indicative of abundant garnet in the residue) and high Sr concentrations (indicative of paucity of feldspar).

#### ACKNOWLEDGMENTS

We gratefully acknowledge important contributions from the following individuals: C. Coath, who provided invaluable assistance in ion probe analyses; Jim Faulds, for sharing his regional expertise; J. Wooden, who performed and shared the first Nd-

Sr-Pb and zircon U-Pb analyses of Ireteba granite; K. Townsend, D. Robinson, and C. Bachl, who provided help and insights in the lab and field; J. Ayers, for general advice and assistance in the research and a review of the thesis on which this article is based; and A. Patiño Douce and M. Dorais, for very helpful reviews of the manuscript. The research was supported by National Science Foundation (NSF) grants EAR-9628380 and 9506551. The University of California, Los Angeles, ion microprobe laboratory is partially supported by a grant from the NSF Instrumentation and Facilities program.

#### REFERENCES CITED

- Allen, C. M.; Wooden, J. L.; Howard, K. A.; Foster, D. A.; and Tosdal, R. M. 1995. Sources of the Early Cretaceous plutons in the Turtle and West Riverside mountains, California: anomalous Cordilleran interior intrusions. *J. Petrol.* 36:1675–1700.
- Anderson, J. L., and Cullers, R. L. 1990. Middle to upper crustal plutonic construction of a magmatic arc: an example from the Whipple Mountains metamorphic core complex. *Geol. Soc. Am. Mem.* 174:47–69.
- Anderson, J. L., and Rowley, M. C. 1981. Syn-kinematic intrusion of peraluminous and associated metaluminous granitic magmas, Whipple Mountains, California. *Can. Mineral.* 19:83–101.
- Bachl, C. A.; Miller, C. F.; Miller, J. S.; and Faulds, J. E. 2001. Construction of a pluton: evidence from an exposed cross-section of the Searchlight pluton, Eldorado Mountains, Nevada. *Geol. Soc. Am. Bull.* 113:1213–1228.
- Beard, B. L., and Glazner, A. F. 1995. Trace element of Sr and Nd isotopic composition of mantle xenoliths from the Big Pine Volcanic Field, California. *J. Geophys. Res.* 100:4169–4179.
- Bennett, V. C., and DePaolo, D. J. 1987. Proterozoic crustal history of the western United States as determined by neodymium isotopic mapping. *Geol. Soc. Am. Bull.* 99:674–685.
- Carl, B. S.; Miller, C. F.; and Foster, D. A. 1991. Western Old Woman Mountains shear zone: evidence for late ductile extension in the Cordilleran orogenic belt. *Geology* 19:893–896.
- Clarke, D. B.; MacDonald, M. A.; and Tate, M. C. 1997. Late Devonian mafic-felsic magmatism in the Meguma Zone, Nova Scotia. *Geol. Soc. Am. Mem.* 191:107–127.
- Daley, E. E., and DePaolo, D. J. 1992. Isotopic evidence for lithospheric thinning during extension: southeastern Great Basin. *Geology* 20:104–108.
- D'Andrea, J. L. 1998. Geology and petrogenesis of the Ireteba Pluton: implications for the generation of peraluminous granites. M.S. thesis, Vanderbilt University, Nashville, Tenn., 104 p.
- Defant, M. J., and Drummond, M. S. 1990. Derivation of some modern arc magmas by melting of young subducted lithosphere. *Nature* 347:662–665.
- Defant, M. J., and Kepezhinskas, P. 2001. Evidence suggests slab melting in arc magmas. *EOS: Trans. Am. Geophys. Union* 82:65–69.
- Defant, M. S.; Richerson, M.; DeBoer, J. Z.; Stewart, R. H.; Maury, R. C.; Bellon, H.; Drummond, M. S.; Feigenson, M. D.; and Jackson, T. E. 1991. Dacite genesis via both slab melting and differentiation: petrogenesis of La Yeguada volcanic complex, Panama. *J. Petrol.* 32:1101–1142.
- Deino, A., and Potts, R. 1992. Age-probability spectra of single-crystal  $^{40}\text{Ar}/^{39}\text{Ar}$  results: examples from Ologesailie, southern Kenya rift. *Quat. Int.* 13/14:47–53.
- DePaolo, D. L. 1981. Neodymium isotopes in the Colorado Front Range and crust-mantle evolution in the Proterozoic. *Nature* 291:193–196.
- DiVincenzo, G.; Andriessen, P. A. M.; and Ghezzi, C. 1996. Evidence of two different components in a Hercynian peraluminous cordierite-bearing granite: the San Basilio Intrusion (central Sardinia, Italy). *J. Petrol.* 37:1175–1206.
- Drummond, M. S., and Defant, M. J. 1990. A model for trondhjemite-tonalite-dacite genesis and crustal growth via slab melting: Archean to modern comparisons. *J. Geophys. Res.* 95:21,503–21,521.
- Dumitru, T. A. 1990. Subnormal Cenozoic geothermal gradients in the extinct Sierra Nevada magmatic arc—consequences of Laramide and post-Laramide shallow-angle subduction. *J. Geophys. Res.* 95:4925–4941.
- Elburg, M. A. 1996a. Evidence of isotopic equilibration between microgranitoid enclaves and host granodiorite, Warburton Granodiorite, Lachlan fold belt, Australia. *Lithos* 38:1–22.
- . 1996b. Genetic significance of multiple enclave

- types in a peraluminous ignimbrite suite, Lachlan fold belt, Australia. *J. Petrol.* 37:1385–1408.
- . 1996c. U-Pb ages and morphologies of zircon in microgranitoid enclaves and peraluminous host granite: evidence for magma mingling. *Contrib. Mineral. Petrol.* 123:177–189.
- Falkner, C. M.; Miller, C. F.; Wooden, J. L.; and Heizler, M. T. 1995. Petrogenesis and tectonic significance of the calc-alkaline, bimodal Aztec Wash pluton, Eldorado Mountains, Colorado River extensional corridor. *J. Geophys. Res.* 100:204–227.
- Farmer, G. L.; Perry, F. V.; Semken, S.; Crowe, B.; Curtis, D.; and DePaolo, D. J. 1989. Isotopic evidence on the structure and origin of subcontinental lithospheric mantle in southern Nevada. *J. Geophys. Res.* 94:7885–7898.
- Faulds, J. E.; Geissman, J. W.; and Mawer, C. K. 1990. Structural development of a major extensional accommodation zone in the Basin and Range Province, northwestern Arizona and southern Nevada: implications for kinematic models of continental extension. *Geol. Soc. Am. Mem.* 176:37–76.
- Foster, D. A., and Fanning, C. M. 1997. Geochronology of the northern Idaho batholith and the Bitterroot metamorphic core complex: magmatism preceding and contemporaneous with extension. *Geol. Soc. Am. Bull.* 109:379–394.
- Foster, D. A., and Hyndman, D. W. 1990. Magma mixing and mingling between syn-plutonic mafic dikes and granite in the Idaho-Bitterroot batholith. *Geol. Soc. Am. Mem.* 174:347–358.
- Fryxell, J. E.; Salton, G. G.; Selverstone, J.; and Wernicke, B. 1992. Gold Butte crustal section, South Virgin Mountains, Nevada. *Tectonics* 11:1099–1120.
- Gardien, V.; Thompson, A. B.; Grujic, D.; and Ulmer, P. 1995. Experimental melting of biotite + plagioclase + quartz  $\pm$  muscovite assemblages and implications for crustal melting. *J. Geophys. Res.* 100:15,581–15,591.
- Gerber, M. E.; Miller, C. F.; and Wooden, J. L. 1995. Plutonism at the eastern edge of the Cordilleran Jurassic magmatic belt, Mojave Desert, California. *Geol. Soc. Am. Mem. Spec. Pap.* 299:351–374.
- Gromet, L. P.; Dymek, R. F.; Haskin, L. A.; and Korotev, R. L. 1984. The “North American shale composite”: its compilation, major and trace element characteristics. *Geochim. Cosmochim. Acta* 48:2469–2482.
- Haapala, I.; Ramo, O. T., and Volborth, A. 1996. Petrogenesis of the Miocene granites of Newberry Mountains, Colorado River Extensional Corridor, southern Nevada. *Geol. Soc. Am. Abstr. Program* 28, no. 7:420.
- Hanchar, J. M.; Miller, C. F.; Wooden, J. L.; Bennett, C.; and Staude, J.-M. 1994. Evidence from xenoliths for a dynamic lower crust, eastern Mojave Desert, California. *J. Petrol.* 35:1377–1415.
- Haskin, L. A.; Wildeman, T. R.; and Haskin, M. A. 1968. An accurate procedure for determination of rare earths by neutron activation. *J. Radioanal. Chem.* 1:337.
- Hodges, K. V., and Walker, J. D. 1992. Extension in the Cretaceous Sevier orogen, North American Cordillera. *Geol. Soc. Am. Bull.* 104:560–569.
- Jahn, B. M.; Glickson, A. Y.; Peucat, J. J.; and Hickman, A. H. 1981. REE geochemical and isotopic data of archaic silicic volcanics and granitoids from the Pilbara block, western Australia: implications for the early crustal evolution. *Geochim. Cosmochim. Acta* 45:1633–1652.
- John, B. E., and Mukasa, S. B. 1990. Footwall rocks to the mid-Tertiary Chemehuevi detachment fault: a window into the middle crust in the southern Cordillera. *J. Geophys. Res.* 95:463–485.
- John, B. E., and Wooden, J. L. 1990. Petrology and geochemistry of the metaluminous to peraluminous Chemehuevi Mountains Plutonic Suite, southeastern California. *Geol. Soc. Am. Mem.* 174:71–98.
- Kontak, D. J., and Clark, A. H. 1997. The Minastira peraluminous granite, Puno, southeastern Peru: a quenched, hypabyssal intrusion recording magma comingling and mixing. *Mineral. Mag.* 61:743–764.
- LeBreton, N., and Thompson, A. B. 1988. Fluid-absent (dehydration) melting of biotite in metapelites in the early stages of crustal anatexis. *Contrib. Mineral. Petrol.* 99:226–237.
- Lee, S. Y.; Barnes, C. G.; Snoke, A. W.; and Howard, K. A. 1997. Geology and petrology of granitic intrusions, Lamoille Canyon, Ruby Mountains, Nevada. *Geol. Soc. Am. Abstr. Program* 29, no. 2:19.
- Martin, H. 1986. Effect of steeper Archean geothermal gradient on geochemistry of subduction-zone magmas. *Geology* 14:753–756.
- . 1999. Adakitic magmas: modern analogues of Archean granitoids. *Lithos* 46:411–429.
- Maxson, J. A., and Tikoff, B. 1996. Hit-and-run collision model for the Laramide Orogeny, western United States. *Geology* 24:968–972.
- McCarthy, T. C., and Patiño Douce, A. E. 1997. Experimental evidence for high-temperature felsic melts formed during basaltic intrusion of the deep crust. *Geology* 25:463–466.
- Metcalf, R. V.; Smith, E. I.; Walker, J. D.; Reed, R. C.; and Gonzales, D. A. 1995. Isotopic disequilibrium among commingled hybrid magmas: evidence for a two-stage magma mixing-commingling process in the Mt. Perkins Pluton, Arizona. *J. Geol.* 103:509–527.
- Miller, C. F. 1985. Are strongly peraluminous magmas derived from mature sedimentary (pelitic) sources? *J. Geol.* 93:673–689.
- Miller, C. F., and Barton, M. D. 1990. Phanerozoic plutonism in the Cordilleran interior, U.S.A. *Geol. Soc. Am. Spec. Pap.* 241:213–231.
- Miller, C. F., and Bradfish, L. J. 1980. An inner Cordilleran belt of muscovite-bearing plutons. *Geology* 8:412–416.
- Miller, C. F.; Fullagar, P. D.; Sando, T. W.; Kish, S. A.; Solomon, G. C.; Russell, G. S.; and Wood-Steltenpohl, L. F. 1997. Low-potassium, trondhjemitic to granodioritic plutonism in the eastern Blue Ridge, southwestern North Carolina–northeastern Georgia. *Geol. Soc. Am. Mem.* 191:235–253.
- Miller, C. F.; Hatcher, R. D., Jr.; Ayers, J. C.; Coath, C. D.; and Harrison, T. M. 2000. Age and zircon inheri-

- tance of eastern Blue Ridge plutons, southwestern North Carolina and northeastern Georgia, with implications for magma history and evolution of the Southern Appalachian Orogen. *Am. J. Sci.* 300: 142–172.
- Miller, C. F., and Meschter, S. M. 2000. Hot and cold granites: evidence from zircon saturation thermometry and inheritance. *Geol. Soc. Am. Abstr. Program* 32, no. 7:A495.
- Miller, C. F.; Watson, E. B.; and Harrison, T. M. 1988. Perspectives on the source, segregation and transport of granitoid magmas. *Trans. R. Soc. Edinb. Earth Sci.* 79:135–156.
- Miller, C. F., and Wooden, J. L. 1994. Anatexis, hybridization and the modification of ancient crust: Mesozoic plutonism in the Old Woman Mountains area, California. *Lithos* 32:111–133.
- Miller, J. S.; Glazner, A. F.; Farmer, G. L.; Suayah, I. B.; and Keith, L. A. 2000. A Sr, Nd, and Pb isotopic study of mantle domains and crustal structure from Miocene volcanic rocks in the Mojave Desert, California. *Geol. Soc. Am. Bull.* 112:1264–1279.
- Muir, R. J.; Weaver, S. D.; Bradshaw, J. D.; Eby, G. N.; and Evans, J. A. 1995. The Cretaceous Separation Point Batholith, New Zealand: granitoid magmas formed by melting of mafic lithosphere. *J. Geol. Soc. Lond.* 152:689–701.
- Mukasa, S. B., and Wilshire, H. G. 1997. Trace-element and Nd-, Sr-, and Pb-isotopic compositions of upper mantle and lower crustal xenoliths, Cima Volcanic Field, California: implications for evolution of the subcontinental lithospheric mantle. *J. Geophys. Res.* 102:20,133–20,148.
- Paces, J. B., and Miller, J. D., Jr. 1993. Precise U-Pb ages of Duluth Complex and related mafic intrusions, northeastern Minnesota: geochronological insights to physical, petrogenetic, paleomagnetic, and tectonomagmatic processes associated with the 1.1 Ga Mid-continent Rift System. *J. Geophys. Res.* 98: 13,997–14,013.
- Patiño Douce, A. E. 1995. Experimental generation of hybrid silicic melts by reaction of high Al-basalt with metamorphic rocks. *J. Geophys. Res.* 100: 15,623–15,639.
- . 1999. What do experiments tell us about the relative contributions of crust and mantle to the origin of granitic magmas? *Geol. Soc. Lond. Spec. Publ.* 168: 55–75.
- Patiño Douce, A. E., and Beard, J. S. 1995. Dehydration-melting of biotite gneiss and quartz amphibolite from 3 to 15 kbar. *J. Petrol.* 36:707–738.
- . 1996. Effects of P,  $f(\text{O}_2)$  and Mg/Fe ratio on dehydration melting of model metagreywackes. *J. Petrol.* 37:999–1024.
- Patiño Douce, A. E., and Harris, N. 1998. Experimental constraints on Himalayan anatexis. *J. Petrol.* 39: 689–710.
- Patrick, D. W., and Miller, C. F. 1997. Processes in a composite, recharging magma chamber: evidence from magmatic structures in the Aztec Wash Pluton, Nevada. *Proc. 30th Int. Geol. Congr. Res. Vol.*, p. 121–135.
- Pitcher, W. S. 1993. *The nature and origin of granite.* London, Chapman & Hall, 321 p.
- Quidelleur, X.; Grove, M.; Lovera, O. M.; Harrison, T. M.; and Yin, A. 1997. Thermal evolution and slip history of the Renbu Zedong Thrust, southeastern Tibet. *J. Geophys. Res.* 102:2659–2679.
- Ramo, O. T.; Haapala, I.; and Volborth, A. 1999. Isotopic and general geochemical constraints on the origin of Tertiary granitic plutonism in the Newberry Mountains, Colorado River Extensional Corridor, Nevada. *Geol. Soc. Am. Abstr. Program* 31, no. 6:A86.
- Rapp, R. P.; Ryerson, F. J.; and Miller, C. F. 1987. Experimental evidence bearing on the stability of monazite during crustal anatexis. *Geophys. Res. Lett.* 14: 307–310.
- Rollinson, H. 1993. *Using geochemical data: evaluation, presentation, interpretation.* New York, Longman Scientific & Technical, copublished with Wiley, 352 p.
- Schuster, R. D., and Bickford, M. E. 1985. Chemical and isotopic evidence for the petrogenesis of the northeastern Idaho Batholith. *J. Geol.* 93:727–742.
- Silva, M. M. V. G.; Neiva, A. M. R.; and Whitehouse, M. J. 2000. Geochemistry of enclaves and host granite from the Nelas area, central Portugal. *Lithos* 50: 153–170.
- Taylor, S. R., and McLennan, S. M. 1981. The composition and evolution of the continental crust: rare earth element evidence from sedimentary rocks. *Philos. Trans. R. Soc. Lond. A* 301:381–399.
- Townsend, K. J.; Miller, C. F.; D'Andrea, J. L.; Ayers, J. C.; Harrison, T. M.; and Coath, C. D. 2000. Low temperature replacement of monazite in the Ireteba granite, southern Nevada: geochronological implications. *Chem. Geol.* 172:95–112.
- Vielzeuf, D., and Montel, J. M. 1994. Partial melting of metagreywackes. 1. Fluid-absent experiments and phase relationships. *Contrib. Mineral. Petrol.* 117: 375–393.
- Watson, E. B. 1996. Dissolution, growth and survival of zircons during crustal fusion: kinetic principles, geological models and implications for isotopic inheritance. *Trans. R. Soc. Edinb. Earth Sci.* 87:43–56.
- Watson, E. B., and Harrison, T. M. 1983. Zircon saturation revisited: temperature and composition effects in a variety of crustal magma types. *Earth Planet. Sci. Lett.* 64:295–304.
- White, A. J. R.; Clemens, J. D.; Holloway, J. R.; Silver, L. T.; Chappell, B. W.; and Wall, J. 1986. S-type granites and their probable absence in southwestern North America. *Geology* 14:115–118.
- Wooden, J. L., and Miller, D. M. 1990. Chronologic and isotopic framework for Early Proterozoic crustal evolution in the eastern Mojave Desert region, SE California. *J. Geophys. Res.* 95:20,133–20,146.
- Wooden, J. L.; Nutman, A. P.; Miller, D. M.; Howard, K. A.; Bryant, B.; DeWitt, E.; and Mueller, P. A. 1994. SHRIMP U-Pb zircon evidence for late Archean and

- early Proterozoic crustal evolution in the Mojave and Arizona crustal provinces. *Geol. Soc. Am. Abstr. Program* 26, no. 6:69.
- Wooden, J. L.; Stacey, J. S.; Howard, K. A.; Doe, B. R.; and Miller, D. M. 1988. Pb isotopic evidence for the formation of Proterozoic crust in the southwestern United States. *In* Ernst, W. G., ed. *Metamorphism and crustal evolution in the western United States*. Englewood Cliffs, N.J., Prentice Hall, p. 68–86.
- Yogodzinski, G. M.; Kay, R. W.; Volynets, O. N.; Koloskov, A. V.; and Kay, S. M. 1995. Magnesian andesite in the western Aleutian Komandorsky region: implications for slab melting and processes in the mantle wedge. *Geol. Soc. Am. Bull.* 107:505–519.